The Most Influenced Community Search on Social Networks

Xueqin Chang[♮], Qing Liu[♮⋆], Yunjun Gao[♮⋆], Baihua Zheng[♯], Yi Cai[‡], Qing Li[†]
[♮]*Zhejiang University,* [⋆]*Zhejiang Key Laboratory of Big Data Intelligent Computing,*
[♯]*Singapore Management University,* [‡]*South China University of Technology,* [†]*The Hong Kong Polytechnic University*
{changxq, qingliucs, gaoyj}@zju.edu.cn, bhzheng@smu.edu.sg, ycai@scut.edu.cn, csqli@comp.polyu.edu.hk

***Abstract*—In this paper, we address a novel problem in social network analysis: the Most Influenced Community Search (MICS). Given a graph and a seed node set S, the MICS problem seeks to identify a densely connected subgraph that is most significantly impacted by S. We formally define MICS, prove its NP-hardness, and show that constant-factor approximation is not feasible. To solve MICS efficiently, we propose a two-phase framework. In the first phase, we compute the influenced expectation for each node, representing its likelihood of being influenced by S. We develop two algorithms: S-InfExp, a sampling-based method with theoretical guarantees, and L-InfExp, a learning-based approach for faster predictions. In the second phase, we introduce two algorithms, GlobalSearch and LocalSearch, to find the most influenced community. GlobalSearch uses a top-down, greedy approach, while LocalSearch applies a bottom-up strategy. Experiments on eight real-world datasets demonstrate that (1) L-InfExp is up to 100× faster than S-InfExp with comparable accuracy, (2) LocalSearch is 10× faster than GlobalSearch, with both algorithms effectively identifying the community with the highest influenced expectations, and (3) our algorithms outperform all baselines.**

***Index Terms*—Influence Propagation, Community Search, Social Network**

I. Introduction

With the proliferation of social networks, millions of people are now connected and interact with each other on a daily basis. This has sparked significant interest in understanding how influence diffuses across these networks [1]–[4]. Researchers and industry professionals have focused on various aspects of influence analysis, such as predicting influence cascades [1], [5]–[8], identifying influential nodes [3], [9]–[14], and maximizing influence spread [2], [15]–[20].

A critical question in this domain is: ***Which users or groups of users are most likely to be influenced by a given set of source users?*** Answering this question is crucial for applications such as targeted marketing [21], epidemic control [22], and personalized recommendation [23]. For example, consider a scenario depicted in Figure 1(a) where a company employs a user v_1 to promote its new product. As v_1's influence propagates through the social network, other users are affected to varying extents, as shown in Figure 1(b). Among them, the highly influenced users $\{v_2, v_3, v_9, v_{10}\}$ form a densely connected subgraph. This subgraph represents a community that is not only the most influenced by v_1 but also features close-knit structure and frequent interactions, which enhances the likelihood of adoption through group dynamics and shared interests. Targeting such a community can significantly boost marketing effectiveness [21]. We refer to this subgraph as the *most influenced community*. Moreover, in practical applications like marketing and political campaigns, the community needs to be of sufficient size, as larger communities are essential for achieving effective outreach [24].

The Most Influenced Community Search Problem. Based on the above motivation, in this paper, we study the novel Most Influenced Community Search (MICS) problem. Specifically, given a directed graph $G(V_G, E_G)$, a size constraint γ, and a set of seed nodes $S \subset V_G$, our goal is to find a subgraph $H \subseteq G$ with $|H| \geq \gamma$ that is most influenced by S and is densely connected. To quantify the impact of S on a community, we introduce the concept of *influenced expectation*, which represents the likelihood of a node being influenced by S. We define the influenced expectation of a community H as the average[1] of the individual influenced expectations of the nodes within H. We employ D-core (a.k.a. (k, l)-core) [26] to assess the structural cohesiveness of the community. The MICS problem has many realistic applications.

Application 1. *During promotional campaigns, companies need to identify receptive user groups for targeted marketing [21]. Partnering with influencers can rapidly promote a new product to a broad audience [27], but narrowing the focus to users most likely to engage with the product (i.e., product users) is essential for boosting sales [28]. Cohesive communities with shared interests and strong intra-group bonding can accelerate product spread, leading to faster purchasing decisions [29]. By applying MICS, companies can pinpoint the community most affected by influencers, where users are not only closely connected to each other, but also have a strong need or interest in the product, thereby optimizing marketing efforts and reducing costs associated with ineffective outreach.*

Application 2. *In infectious disease outbreaks, cohesive communities, such as neighborhoods or workplaces, often share similar lifestyles and health behaviors, which can accelerate the spread of disease [22]. For health organizations like the CDC, identifying the most influenced (i.e., the highest-risk) community is essential for controlling outbreaks. MICS can pinpoint the community most affected by an outbreak, enabling efficient tracing, analysis, and resource allocation [30]. Targeting the most influenced communities first allows better prevention and control, reducing transmission risk and improving outbreak management.*

Challenges and Solutions. To effectively and efficiently address the MICS problem, we propose a two-phase framework.

The first phase is to compute the influenced expectation of each node for a given seed set S. This involves determining the likelihood that each node will be affected by S. However, calculating the exact influenced expectations is $\#\mathbf{P}$-hard. Moreover, advanced Reverse Influence Sampling (RIS) [16]

[1]The influenced expectation of a graph can be defined using other aggregation functions such as *percentiles*, *min*, *max*, and *sum*. For a detailed discussion, please refer to our technical report [25].

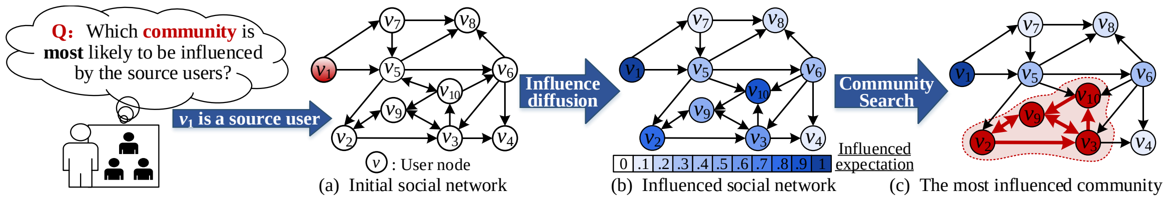

(a) Initial social network (b) Influenced social network (c) The most influenced community

Fig. 1: A motivating example

is not applicable to our problem for three key reasons: **(i)** RIS is designed to compute the influence spread of S, which differs from our task; **(ii)** RIS does not concern which specific nodes are influenced; and **(iii)** The unbiased estimator in RIS cannot be applied to estimate influenced expectation of each node. Additionally, Monte Carlo Simulation [27] has higher complexity, making it impractical for large graphs, as demonstrated in Section VII. Thus, we develop two novel algorithms to efficiently calculate influenced expectations for nodes in G, based on a given seed set S.

We firstly propose S-InfExp, which estimates the influenced expectation of each node with theoretical guarantees. S-InfExp generates an unbiased estimation of influenced expectations by randomly sampling multiple *forward influence propagation instances* from the given seed set S. However, directly traversing the whole graph to generate each instance incurs significant time overhead. To address this challenge, we propose a novel *subset sampling technique*, which models the propagation of each activated node to its out-neighbors as discrete distribution sampling [31]. Specifically, we define pivotal nodes and utilize edge weights to determine a skip distance (i.e., the number of out-neighbors to skip after each pivotal node) based on a geometric distribution. This approach allows us to skip certain out-neighbors during the generation of each influence propagation instance, significantly improving sampling efficiency. Based on S-InfExp, we develop the learning-based algorithm L-InfExp to further improve the efficiency. L-InfExp can adopt various nonlinear regression models to predict the influenced expectation for each node online without generating influence propagation instances. This significantly reduces computation time and enables real-time analysis.

The second phase involves identifying the most influenced community based on the influenced expectations from the first phase. Existing studies [32]–[40] on the influential community search assume either no size constraint or a specified size limit, limiting their practical applicability. To address this, we introduce the *most influenced community (MIC)* model, which ensures the community size meets or exceeds a threshold for meaningful real-world outcomes (e.g., higher adoption rates or broader social impact) [24]. We prove that finding the *MIC* is **NP**-hard and inapproximable within a constant factor. Thus, directly applying existing enumerative methods [32], [36], [38], [40] to address our problem would be computationally prohibitive. To overcome this, we propose two new algorithms for the second phase.

We firstly propose GlobalSearch. We show that the graph's influenced expectation function is non-monotonic and non-submodular, meaning removing a node from a community D to form another D' can either increase or decrease the influenced expectation. This non-linearity complicates the decision-making process regarding which node to remove to uncover a community with a higher influenced expectation in each iteration. To tackle this challenge, we propose *two heuristic strategies* to greedily remove the nodes within GlobalSearch. Moreover, we present LocalSearch, which sorts nodes by their influenced expectations in descending order. Starting with the node having the largest influenced expectation, LocalSearch identifies the *local most influenced community* containing that node. The process is repeated by removing the node and searching for the local most influenced community for the next highest node. The community with the maximum influenced expectations is ultimately selected. Various pruning techniques are also incorporated to enhance efficiency.

Contributions. Our contributions are summarized as follows.

- We investigate the most influenced community search problem in social networks for the first time.
- We propose a sampling-based algorithm, S-InfExp, to estimate the influenced expectations with theoretical guarantees. Additionally, we develop a learning-based method, L-InfExp, for efficient prediction of influenced expectations.
- We design GlobalSearch and LocalSearch algorithms to identify the most influenced community, incorporating various pruning strategies to improve search efficiency.
- We conduct extensive experiments on eight real networks to demonstrate the effectiveness, efficiency, and scalability of the proposed algorithms.

Roadmap. Section II reviews the related work. Section III defines and analyzes the problem of MICS. Section IV provides an overview of proposed techniques. Section V presents S-InfExp and L-InfExp algorithms. Section VI introduces GlobalSearch and LocalSearch algorithms. Section VII reports experimental result and Section VIII concludes the paper.

II. Related Work

Community Search. Community search aims to find cohesive subgraphs containing given query nodes [41]. It has been widely studied across different graph types, including directed graphs [26], [42], [43], attributed graphs [44]–[46], and heterogeneous graphs [47], [48]. Recently, learning-based algorithms have been proposed for community search [49], [50].

The most closely related community search to our work is influential community search [32]–[40], which aims to find top-r communities with the highest influence scores. However, influential community search differs from our problem in two key aspects. First, in influential community search, the nodes' influence scores are typically given in advance and are fixed. In contrast, our problem requires computing the influenced expectation for each node under a given set of seed nodes. Second, Our problem sets a lower bound on community size, while influential community search sets an upper bound or no bound. Therefore, techniques designed for influential community search cannot be directly applied to our problem.

Community Detection. Community detection aims to retrieve all communities that meet specific constraints [51]–[53]. Recent studies have employed clustering techniques for community detection [54]–[56]. However, these works did not require structural or size constraints of community answers, nor do they consider the effects of influence propagation, which is the focus of our MICS problem in this paper.

Influence Analysis. Influence analysis has been extensively studied in social networks and includes topics such as influence cascade prediction [1], [5]–[8], influential nodes identification [3], [9]–[14], and influence maximization [2], [15]–[20], [57], [58]. In this paper, we introduce a new perspective in influence analysis, finding the most influenced community for a given seed node set. The Restricted Maximum Probability Path (RMPP) [59], used in previous work [60] to estimate seed nodes' influence spread. However, using the RMPP to compute the influenced expectation of each node poses two main issues. **(i)** The RMPP represents the path with the maximum influence probability from a seed node s to a node u, implying that influence propagates along this highest probability path, which does not align with the realistic influence propagation process. **(ii)** The RMPP only considers the maximum probability path, which can result in biased estimates by overlooking other potential influence paths.

III. Preliminaries

In this section, we formally define and analyze the most influenced community search (MICS) problem.

A. Problem Formulation

We consider a directed graph $G(V_G, E_G)$, where V_G and E_G represent the sets of n nodes and m edges, respectively. In our work, we focus on directed graphs that have been encrypted or anonymized for privacy concerns. Each directed edge $e = (u, v) \in E_G$ is associated with an influence weight $w(u, v) \in [0, 1]$, which quantifies the influence of node u on node v. In this context, u is referred to as an in-neighbor of v, and v is an out-neighbor of u. For a node $v \in V_G$, let $N_G^{in}(v)$ (resp. $N_G^{out}(v)$) denote the set of in-neighbors (resp.out-neighbors) of v. Correspondingly, the in-degree of v, denoted by $d_G^{in}(v) = |N_G^{in}(v)|$, represents the number of in-neighbors of v in G. Similarly, the out-degree of v, denoted by $d_G^{out}(v) = |N_G^{out}(v)|$, represents the number of out-neighbors of v in G. To define the MICS problem, we introduce the cohesive subgraph model and influence propagation model.

Cohesive subgraph model. In this paper, we employ the D-core (a.k.a. (k,l)-core) to measure community structure density for two key reasons. **(i)** We model the social network as a directed graph, as in previous works [15], [17]–[19]. Unlike the k-core [61], [62] and k-truss [63], [64], which are designed for undirected graphs, the D-core is tailored for directed graphs [26], [43]. **(ii)** The D-core is computationally efficient compared to other community models [65].

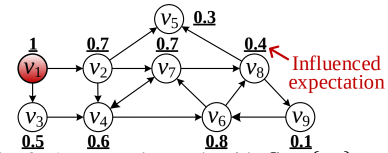

Fig. 2: An example graph with $S = \{v_1\}$

Definition 1. (D-core) [26]. *Given a directed graph $G(V_G, E_G)$, two integers k and l, a subgraph $H(V_H, E_H) \subseteq G$ is a D-core of G, if it satisfies the following conditions:*

1) ***Cohesive:*** $\forall v \in V_H$, $d_H^{in}(v) \geq k$ *and* $d_H^{out}(v) \geq l$.
2) ***Maximal:*** *For any subgraph $H' \subseteq G \wedge H' \supset H$ that contains H, H' is not a D-core.*

According to Definition 1, a D-core satisfies both cohesive and maximal constraints. Based on this, we define the $\tilde{D}$-core (a.k.a. $(\tilde{k}, \tilde{l})$-core) as a subgraph that satisfies only the cohesive constraint. For example, in Figure 2, the directed subgraph H_1 induced by nodes v_6, v_8, and v_9 is a $(\tilde{1}, \tilde{1})$-core because $\forall v \in V_{H_1}$, $d_{H_1}^{in}(v) = d_{H_1}^{out}(v) = 1$, but it is not maximal.

Influence propagation model. We employ the Independent Cascade (IC) model [27] to simulate influence propagation, as it is widely adopted to depict this process [15], [20]. In the IC model, for a given seed node set $S \subset V_G$, the influence propagation process unfolds in discrete steps as follows. At step 0, all nodes in S are activated, while the remaining nodes remain inactive. Once a node is activated, it stays activated throughout the propagation process. In each subsequent step, if a node u is activated at step i, it has a single chance to activate each of its inactive out-neighbors $v \in N_G^{out}(u)$ with a probability determined by the influence weight $w(u, v)$ at step $i+1$. After this attempt, u cannot activate any additional nodes. The process continues until no more nodes can be activated.

Based on the influence propagation model, for each node $v \in V_G$, we define the influenced expectation as follows.

Definition 2. (Influenced expectation). *Given a directed graph $G(V_G, E_G)$ and a seed node set $S \subset V_G$, for each node $v \in V_G$, we define $Ie(v, S)$ as the influenced expectation of v, which represents the probability that v will be activated by S under the IC model.*

For instance, in Figure 2, v_1 is the seed node (i.e., $S = \{v_1\}$), and numbers next to vertices represent their influenced expectations under the current seed node set S. For example, $Ie(v_8, \{v_1\}) = 0.4$ indicates that there is a 40% chance of v_8 being activated by v_1. For a subgraph $H(V_H, E_H) \subseteq G$, we define the influenced expectation of H as follows.

Definition 3. (Influenced expectation of H). *Given a directed graph G, a subgraph $H(V_H, E_H) \subseteq G$, and a seed node set $S \subset V_G$, the influenced expectation of H, denoted by $Ie(H, S)$, is the average expectation that H is influenced by S under the IC model. Specifically, $Ie(H, S) = \frac{\sum_{v \in V_H} Ie(v,S)}{|V_H|}$.*

In Definition 3, $Ie(H, S)$ is defined as the average of the influenced expectations of all nodes in H. Note that $Ie(H, S)$ could also be defined using other aggregate functions, such as *percentile*, *min*, *max*, or *sum*. In real-world scenarios, users can choose the most appropriate aggregate function based on the specific context, as our framework can be easily extended to handle these alternatives.

Based on the above definitions, we introduce a novel community model called the most influenced community (MIC).

Definition 4. (MIC). *Given a directed graph $G(V_G, E_G)$, a seed node set $S \subset V_G$, and integers k and l, a subgraph $H(V_H, E_H) \subseteq G$ is an MIC if it satisfies:*

1) ***Cohesive:*** *$\forall v \in V_H$, $d_H^{in}(v) \geq k$ and $d_H^{out}(v) \geq l$.*
2) ***Connected:*** *H is a connected subgraph.*
3) ***Most influenced:*** *H has the maximum influenced expectation $Ie(H, S)$ among all the subgraphs that satisfy above two conditions.*
4) ***Maximal:*** *There is no other subgraph $H' \subseteq G \wedge H' \supset H$ that satisfies conditions 1), 2), and 3).*

In summary, the MIC is a connected $\tilde{D}$-core with the highest influence expectation and that is also maximal at the same influenced expectation. Then, we define the MICS problem.

Problem 1. (MICS). *Given a directed graph $G(V_G, E_G)$, a seed node set $S \subset V_G$, two integers k and l, and a size constraint γ, the objective of MICS problem is to find the MIC with $|MIC| \geq \gamma$.*

The size constraint γ ensures that the community is large enough for practical applications, as discussed in Section I.

Example 1. *Figure 2 shows a directed graph G. Let $S = \{v_1\}$, $\gamma = 2$, $k = 1$, and $l = 1$. The number next to each node is its influenced expectation w.r.t., S. The directed subgraph H_1 induced by nodes v_4, v_6, and v_7 is a MIC with a maximum influenced expectation $Ie(H_1, \{v_1\}) = (0.6+0.8+0.7)/3 = 0.7$ and $|MIC| \geq 2$. Hence, H_1 is the result of MICS.*

B. Problem Analyses

In this section, we demonstrate the NP-hardness of the MICS problem by breaking it down into two sub-problems.

Problem 2. (IEC). *Given a directed graph $G(V_G, E_G)$ and a seed node set $S \subset V_G$, the problem of Influenced Expectation Computation (IEC) is to compute the influenced expectation $Ie(v, S)$ for every node $v \in V_G$.*

Problem 3. (CS). *Given a directed graph $G(V_G, E_G)$, two integers k and l, a size constraint γ, and the influenced expectation $Ie(v, S)$ for every node $v \in V_G$, the problem of Community Search (CS) is to find the MIC with $|MIC| \geq \gamma$.*

For Problems IEC and CS, we have the following theorems.

Theorem 1. *The IEC is #P-hard under the IC model.*

Proof. We prove this theorem by a reduction from the Probabilistic s-t Connectivity (PC) problem in a directed graph [66]. Specifically, give a directed graph $G(V_G, E_G)$, where each edge has an existence probability of 0.5, and two nodes $s \in V_G$ and $t \in V_G$, the PC problem is to compute the probability that s is connected to t. According the PC problem, we set up the IEC problem on G as follows: (1) the influence weights of all edges are set to 0.5; (2) $S = \{s\}$; and (3) $v = t$. Clearly, t is influenced by s if and only if there is a directed path from s to t. Thus, the probability that s is connected to t equals $Ie(t, s)$. Since the PC problem is #P-complete [66], the IEC problem is also #P-hard. □

Theorem 1 shows the hardness of computing exact influenced expectation. Therefore, in Section V, we develop approximation algorithms to estimate the influenced expectation $Ie(v, S)$ for each node $v \in V_G$ w.r.t. a given set of seed nodes S. Assuming we have computed the influenced expectation of each node, we show that searching the MIC is NP-hard with no constant-factor approximation.

Theorem 2. *The CS problem is NP-hard.*

Proof. We prove this by reducing the Decision of the Maximum Clique (DMC) problem to the CS problem. Specifically, given an undirected graph $G'(V', E')$ and an integer k', the DMC is to determine whether G' contains a k'-clique. Based on the DMC, we construct a directed graph $G(V, E)$ for the CS problem as follows: (1) $V = V'$; (2) $\forall u, v \in V'$, if there exists an edge between u and v in E', add both (u, v) and (v, u) to E; (3) add a new vertex $w \notin V'$ to V, and $\forall v \in V'$, add both (w, v) and (v, w) to E; (4) set $Ie(w, S)$ to a positive integer, while for the remaining vertices in V, $Ie(v, S)$ is set to 0. We set the parameters of the CS problem as: $k = l = \gamma = k' + 1$. If there exists a polynomial-time algorithm for the CS problem, we could solve the DMC. Specifically, let H be the community returned by the CS problem. Then, the influenced expectation of H is $Ie(H, S) = \frac{Ie(w,S)}{|H|}$. To maximize $Ie(H, S)$, $|H|$ should be minimized. The smallest possible $|H|$ is $k' + 1$. However, if $|H| = k' + 1$, the subgraph of G' induced by $\{V_H - w\}$ is a k'-clique. Otherwise, G' does not contain a k'-clique. This contradicts the fact that the DMC problem is NP-complete. Thus, the CS problem is NP-hard. □

Theorem 3. *There are no constant-factor approximation algorithms for the CS problem.*

Proof. As demonstrated by Amini et al. [67], for $r \geq 3$, the problem of finding the minimum subgraph where each vertex's degree is at least r (SMSMD$_r$) does not exist any constant-factor approximation, unless $P = NP$. As shown in Theorem 2, the CS problem requires minimizing $|H|$. If we set $k = l = r$ and $\gamma = 0$, the CS problem is equivalent to SMSMD$_r$ problem. Consequently, there are no constant-factor approximation algorithms for the CS problem. □

Based on Theorems 1, 2, and 3, we can conclude that the MICS problem is NP-hard.

Theorem 4. *The MICS problem is NP-hard, and no constant-factor approximation algorithms exist for it.*

Next, we analyze the objective function $Ie(H, S)$ for the MICS problem, where H is a D-core of size at least γ.

Theorem 5. *$Ie(H, S)$ is non-monotonic and non-submodular*[2].

Due to the non-monotonicity and non-submodularity of $Ie(H, S)$, existing greedy and other approximation algorithms designed for monotonic and submodular objective functions are not applicable to our problem.

IV. Framework Overview

To address the MICS problem, we propose a framework illustrated in Figure 3, which comprises two main phases:

[2]Due to the space limitation, all the omitted proofs are moved to [25].

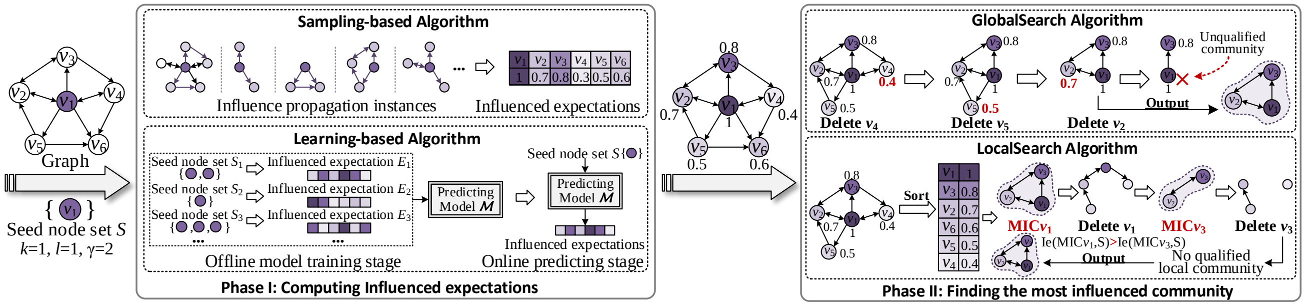

Fig. 3: Framework overview

- Phase I involves computing the influenced expectation for each node, a task proven to be #P-hard as shown in Theorem 1. To address this, we present two novel algorithms. S-InfExp is to randomly sample a sufficient number of forward influence propagation instances to unbiasedly estimate the influenced expectation of each node. Based on the influenced expectations obtained from S-InfExp, L-InfExp applies nonlinear regression models to predict the influenced expectation for each node, which can significantly improve the efficiency.
- Phase II focuses on retrieving the most influenced community that satisfies specific degree and size constraints. Given the NP-hardness of the CS problem, we design two new algorithms. GlobalSearch finds the community in a top-down manner by iteratively removing the node with the smallest influenced expectation. In contrast, LocalSearch identifies the community in a bottom-up manner by finding the community containing node v that has the maximal influenced expectation for each $v \in V_G$.

In the subsequent two sections, we will provide detailed descriptions of the algorithms used in Phases I and II.

V. Influenced Expectation Computation

In this section, we propose a sampling-based algorithm S-InfExp to approximate the influenced expectation of each node with theoretical guarantee, followed by a learning-based method L-InfExp for predicting these expectations.

A. Sampling-based Algorithm

In Section III-A, we introduced the IC model to simulate influence propagation. The propagation process can be characterized as the live edge procedure [27]. Specifically, by removing each edge (u, v) with $1 - w(u, v)$ probability, the remaining graph is referred to as an influence propagation instance. Building on this, we define the concept of influence propagation instance as follows.

Definition 5. (Influence propagation instance). *Given a directed graph $G(V_G, E_G)$, a seed node set $S \subset V_G$, and a subgraph $g \subseteq G$, g is considered an influence propagation instance w.r.t. S if it satisfies: (1) g contains S, (2) for every vertex $v \in V_g - S$, there exists a successful propagation path from a seed node $s \in S$ to v within g, and (3) for every vertex $w \in V_G - V_g$, no path exists from $s \in S$ to w.*

Intuitively, for a given seed set S, an influence propagation instance g represents a scenario where all vertices in g are activated by S, while vertices outside g are not activated. We denote (1) $p(g)$ as the existence probability of g, which is $p(g) = \prod_{e \in E_g} w(e) \prod_{e \in (E_G - E_g)} 1 - w(e)$, and (2) $\mathcal{G}$ as the set of all influence propagation instances w.r.t. S. $Ie(v, S)$ is the expectation of v being activated by S, computed as follows.

$$Ie(v, S) = \sum\nolimits_{g \in \mathcal{G} \wedge v \in V_g} p(g). \quad (1)$$

In other words, $Ie(v, S)$ is the sum of the existence probabilities of the influence propagation instances that include v. Computing $Ie(v, S)$ directly by enumerating all influence propagation instances is computationally prohibitive. Instead, we use sampling technique to sample partial influence propagation instances to estimate $Ie(v, S)$. This involves addressing three main issues: (1) How to estimate $Ie(v, S)$ from sampled influence propagation instances, (2) How to sample influence propagation instances, and (3) How to ensure the accuracy of the estimated $Ie(v, S)$.

Estimating $Ie(v, S)$ from Sampled Influence Propagation Instances. Given a set of independent influence propagation instances $\mathcal{I} = \{I_1, I_2, \cdots\}$ originating from the seed node set S on graph $G(V_G, E_G)$, the estimate of v's influenced expectation, denoted by $\tilde{I}e(v, S)$, is given by

$$\tilde{I}e(v, S) = \frac{|\{I | I \in \mathcal{I} \wedge v \in V_I\}|}{|\mathcal{I}|}. \quad (2)$$

In essence, we employ the proportion of sampled instances in $\mathcal{I}$ that include v as an estimate for $Ie(v, S)$.

Sampling Influence Propagation Instances. A straightforward method is to traverse the graph based on the IC model. Starting from the seeds, we activate them and explore their out-neighbors. For each unactivated out-neighbor v of an activated node u, a random number between 0 and 1 is generated. If it exceeds the influence weight $w(u, v)$, v is activated, as shown in Figure 4(a). This process repeats until no more nodes can be activated. The induced subgraph of activated vertices forms an influence propagation instance. Generating each instance takes $O(\sum_{u \in V_G} d_G^{out}(u)) = O(|E_G|)$ time, and sampling a set of instances $\mathcal{I}$ requires $O(|\mathcal{I}| \cdot |E_G|)$ time.

To enhance efficiency, we propose a *subset sampling technique*, where the propagation of each activated node to its out-neighbors is modeled as discrete distribution sampling [31] during the generation of each influence propagation instance. Specifically, for an activated node u with t out-neighbors v_1, $\cdots$, v_t where $t = d_G^{out}(u)$, we first sort the out-neighbors by their influence weights $w(u, v)$ in descending order. We then select a node to activate in two steps. (1) We choose the first node v' as the pivotal node and use $w(u, v')$ to determine

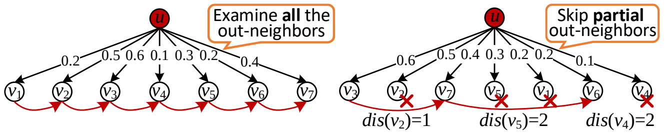

(a) Original sampling method (b) Subset sampling method

Fig. 4: Illustrations of sampling methods

a skip distance $dis(v')$ based on a geometric distribution $G(w(u,v'))$, where $dis(v') = \left\lfloor \frac{\log(rand())}{\log(1-w(u,v'))} \right\rfloor$ denotes the number of nodes skipped during the sampling. (2) We select the $dis(v')$-th node after v', denoted v''. To ensure v'' is activated with probability $w(u,v'')$, we sample a random number $R \in [0,1)$ and activate v'' if $R \leq \frac{w(u,v'')}{w(u,v')}$. Then, the node after v'' is set as the pivotal node for the next node selection. This process continues until no more nodes v'' can be selected. According to [31], for a node u, subset sampling for discrete distributions achieves an expected time complexity of $O(1+\kappa+\log d_G^{out}(u))$, where $\kappa = \sum_{v \in N_G^{out}(u)} w(u,v)$. Figure 4(b) illustrates subset sampling method, showing the skipped vertices v_2, v_5, v_1, and v_4.

Ensuring Estimate Quality. To ensure that $\tilde{I}e(v,S)$ is an unbiased estimate of $Ie(v,S)$, we extend *chernoff inequalities* [68] to analyze the required sample size $|\mathcal{I}|$.

Theorem 6. *Given a directed graph $G(V_G, E_G)$ and a seed set $S \subset G$, for any node $v \in V_G$, the estimate $\tilde{I}e(v,S)$ derived via subset sampling satisfies $|\tilde{I}e(v,S) - Ie(v,S)| < \epsilon \cdot Ie(v,S)$ with probability of at least $(1-n^{-l})$ when $|\mathcal{I}| \geq \frac{l\cdot(2+\epsilon)\cdot\log n}{\epsilon^2 \cdot Ie(v,S)}$, where $n = |V_G|$, $\epsilon \in (0,1)$ is a user-defined parameter, and l is chosen to ensure a success probability of $1-\frac{1}{n}$.*

Theorem 6 offers a theoretical bound on the required sample size. As the number of samples increases, the biases in the estimated influenced expectation decrease, staying within the ϵ bound. By the law of large numbers, in practice, as $|\mathcal{I}|$ increases, $\tilde{I}e(v,S)$ converges to $Ie(v,S)$, but at a higher cost.

S-InfExp Algorithm. We propose a sampling-based algorithm, S-InfExp, to compute the influenced expectation for every node. Algorithm 1 provides the pseudo code. S-InfExp begins by initializing $I(v)$ for each node v, which tracks the number of influence propagation instances containing v (Line 1). It then generates α influence propagation instances (Lines 2-17). For each instance, S-InfExp initializes an empty queue Q and marks all nodes as unactivated (Line 3). All the seed nodes are activated and added to Q (Line 4). S-InfExp performs a BFS traversal of the activated nodes. For each activated node u, S-InfExp sorts u's out-neighbors in descending order of their influence weights and sets the first node as the pivotal node (Lines 7-9). Then, S-InfExp utilizes the subset sampling technique to select u's out-neighbors to activate (Lines 10-16). After generating α influence propagation instances, S-InfExp computes the influenced expectation $\tilde{I}e(v,S)$ for each node and finally returned them (Lines 18-19).

Time Complexity. The time cost for generating an influence propagation instance is $O(\sum_{u \in V_G} \log d_G^{out}(u)) = O(|V_G| \log(|V_G|))$, and the overall complexity of S-InfExp is $O(\alpha \cdot |V_G| \log(|V_G|))$. To reduce running time, we can relax the accuracy requirement, decreasing the number of samples needed.

Algorithm 1 S-InfExp

Input: a graph $G(V_G, E_G)$, a seed set S, and a sample size α
Output: $\tilde{I}e(v,S)$ for $\forall v \in V_G$
1: **for** each $v \in V_G$ **do** $I(v) \leftarrow 0$;
2: **for** $j \leftarrow 1$ to α **do**
3: Queue $Q \leftarrow \emptyset$; Mark $\forall v \in V_G$ as unactivated;
4: **for** each $s \in S$ **do**
5: Mark s as activated; Add s to Q; $I(s) \leftarrow I(s)+1$;
6: **while** $Q \neq \emptyset$ **do**
7: Pop u from Q;
8: Sort u's out-neighbors by descending influence weight;
9: $v' \leftarrow$ The first out-neighbor of u;
10: **for** $i \leftarrow 0$; $i < d_G^{out}(u)$; $i++$ **do**
11: $dist(v') \leftarrow \lfloor log(rand())/log(1-w(u,v')) \rfloor$;
12: $i \leftarrow i + dist(v')$;
13: **if** $i \geq d_G^{out}(u)$ **then break**;
14: $v'' \leftarrow$ the $dist(v')$-th out-neighbor after v';
15: **if** $rand() \leq w(u,v'')/w(u,v') \wedge v''$ is inactive **then**
16: $I(v'')++$; Insert v'' into Q; Mark v'' as activated;
17: $v' \leftarrow$ the node after v'';
18: **for** each $v \in V_G$ **do** $\tilde{I}e(v,S) \leftarrow I(v)/\alpha$;
19: **Return** $\cup_{v \in V_G} \tilde{I}e(v,S)$.

B. Learning-based Algorithm

While S-InfExp is effective for computing influenced expectations, its time complexity can be prohibitive for real-time analysis due to the need for multiple graph traversals. To address this, we propose a learning-based algorithm, L-InfExp, which predicts the influenced expectation for each node without requiring generating influence propagation instances. L-InfExp operates on the following principle: Given a graph G, we randomly select seed node sets $\mathcal{S} = \{S_1, S_2, ...\}$ and use S-InfExp to compute the influenced expectations $\mathcal{E} = \{\varepsilon_1, \varepsilon_2, ...\}$ for these sets. The seed node sets $\mathcal{S}$ and their corresponding influenced expectations $\mathcal{E}$ serve as training data for a predictive model. As the training data size increases, the model can predict the influenced expectations more accurately. Once trained, this model can quickly predict the influenced expectations of nodes for a new seed node set based on the learned patterns and characteristics of the seed node set, significantly reducing computation time and enabling online analysis.

The workflow of L-InfExp is illustrated in Figure 5, which consists of two stages, offline model training and online prediction of influenced expectation. In the offline model training stage, we generate training data, which includes seed node sets and their corresponding influenced expectations. Using this data, we train a predictive model to estimate influenced expectations. This stage produces a trained model for future predictions. In the online predicting stage, for a given seed set S, we encode S into a multi-hot vector and input it to the trained model to predict the influenced expectation for each node. Next, we present a few key components of L-InfExp.

Model selection. For predicting influenced expectations, we use nonlinear regression techniques. Specifically, nonlinear regression is a type of regression analysis to model the complex relationships between dependent and independent variables. In our case, $Ie(v,S) = f_v(x_{v_1}, x_{v_1}, \cdots, x_{v_n}) + \epsilon$, where x_{v_i} indicates whether node v_i is in the given seed node set S, and f_v predicts $Ie(v,S)$ for node v. Hence, our task is to train f_v for each node v. Various models can be used for nonlinear regression, such as Random Forest [69], Decision Tree [70], and k-Nearest Neighbor models [71]. It is worth noting that

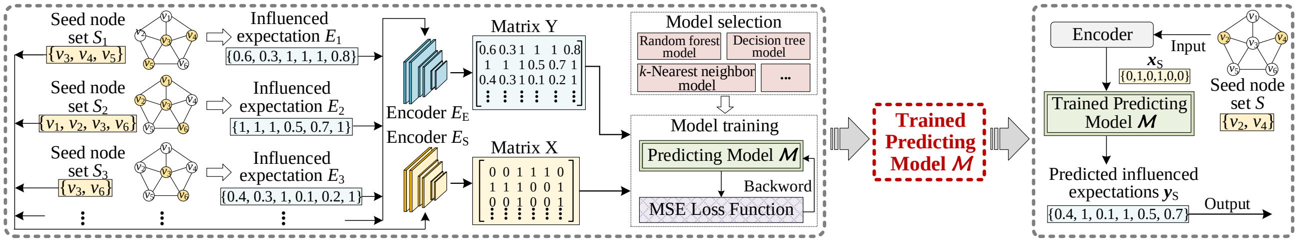

(a) Offline model training stage (b) Online predicting stage

Fig. 5: The workflow of L-InfExp

L-InfExp can adopt any of the aforementioned models. We evaluate and compare these models in our experiments. For simplicity, we denote the predictive model as $\mathcal{M}$.

Encoders. The training data consists of two parts: the seed node sets $\mathcal{S}$ and their corresponding influenced expectations sets $\mathcal{E}$. Each seed node set $S_i \in \mathcal{S}$ is encoded as a multi-hot vector $\boldsymbol{x}_i \in \{0,1\}^n$ where $n = |V_G|$. If $v_j \in S_i$, $\boldsymbol{x}_i[j] = 1$. Otherwise $\boldsymbol{x}_i[j] = 0$. Take the graph G with $|V_G| = 11$ plotted in Figure 2 as an example. For the seed node set $S = \{v_3, v_5, v_{10}\}$, the encoded vector is $\boldsymbol{x} = [0,0,0,1,0,1,0,0,0,0,1]$. In addition, each influenced expectations set $E_i \in \mathcal{E}$ w.r.t., S_i is encoded as a probability vector $\boldsymbol{y}_i \in [0,1]^n$, where $\boldsymbol{y}_i[j]$ represents the influenced expectation for node v_j w.r.t. S_i. Let $|\mathcal{S}| = |\mathcal{E}| = \beta$. We encode all seed nodes sets $\mathcal{S}$ and their corresponding influenced expectations $\mathcal{E}$ into multi-hot matrices X and Y, respectively, where

$$X = [\boldsymbol{x}_1, \boldsymbol{x}_2, \cdots, \boldsymbol{x}_\beta]^\top, Y = [\boldsymbol{y}_1, \boldsymbol{y}_2, \cdots, \boldsymbol{y}_\beta]^\top. \quad (3)$$

Then, matrices X and Y are employed to train $\mathcal{M}$ by minimizing the loss function.

Loss function. We adopt the Mean Squared Error (MSE) to assess the model's performance: minimize the MSE between the predicted influenced expectations $\hat{\boldsymbol{y}}_i \in [0,1]^n$ and the ground-truth influenced expectations $\boldsymbol{y}_i \in [0,1]^n$ for each seed node set $S_i \in \mathcal{S}$, where $\hat{\boldsymbol{y}}_i[j]$ is the predicted influenced expectation of node v_j, and $\boldsymbol{y}_i[j]$ denotes the ground-truth influenced expectation of node v_j. The loss function can be expressed as follows:

$$\min \mathcal{L} = \frac{1}{\beta} \sum\nolimits_{i=1}^{\beta} \|\hat{\boldsymbol{y}}_i - \boldsymbol{y}_i\|_2 \quad (4)$$

Online prediction. During the online influenced expectation prediction stage, we encode the given seed node set S into a multi-hot vector $\boldsymbol{x}_S \in \{0,1\}^n$, which is then input into the trained model $\mathcal{M}$ to obtain the vector $\boldsymbol{y}_S$, which represents the predicted influenced expectations for all nodes.

Time Complexity. We employ Random Forest in L-InfExp due to its superior predictive performance, as demonstrated in Section VII-A. Then, the overall complexity of the offline model training stage is $O(\beta \cdot \alpha \cdot |V_G| \log(|V_G|)) + O(\beta \cdot |V_G|) + O(T \cdot \beta \cdot \sqrt{|V_G|} \cdot d)$. The online prediction complexity is $O(|V_G|) + O(T \cdot |V_G| \cdot d)$, where T and d are the Random Forest model's hyperparameters. Further details are in [25].

C. Discussion

There are many other diffusion models, such as Linear Threshold (LT) model [27] and Invitation Mechanism (IM) model [72]. We discuss whether S-InfExp and L-InfExp can be applied to these diffusion models. Specifically, both the IC and LT models share the same discrete-time cascade process. For the LT model, the edge sampling probability is proportional to its weight, making S-InfExp applicable. However, for the IM model, the propagation success depends on whether the target user accepts the source user's invitation, rather than on edge weight. This key difference renders S-InfExp inapplicable to the IM model. On the other hand, once the influenced expectations of seed node sets are obtained under any influence diffusion model, L-InfExp can predict the influenced expectation of each node for any given seed set. Therefore, L-InfExp is applicable to both LT and IM models.

VI. MIC Search

After computing the influenced expectation of each node for a given seed set, in this section, we propose GlobalSearch and LocalSearch to identify the most influenced community.

A. Global Search Algorithm

According to Definition 4, the MIC is a connected $\tilde{D}$-core (i.e., a subgraph that satisfies only the cohesive constraint) with the highest influenced expectation and is also maximal at the same influenced expectation. Our goal is to identify such a subgraph with a size of at least γ. However, the challenge lies in finding the connected $\tilde{D}$-core with the maximum influenced expectation. As demonstrated in Theorem 5, the function $Ie(H,S)$ is non-monotonic and non-submodular, meaning that removing a vertex from H to form another $\tilde{D}$-core H' can either increase or decrease $Ie(H',S)$. Hence, we need to check all possible connected $\tilde{D}$-cores contained within H to find the one with the maximum influenced expectation. Clearly, enumerating all such $\tilde{D}$-cores for a given H (with n_H nodes and m_H edges) is computationally expensive. This is because enumerating all subgraphs of H generates at most 2^{n_H} subgraphs, and verifying whether each subgraph satisfies the cohesive and connectivity constraints has a worst-case complexity of $O(n_H + m_H)$. Thus, the overall time complexity is $O(2^{n_H}(n_H + m_H))$, making it highly computationally expensive for large graphs. To address this challenge, we propose two greedy strategies to find the connected $\tilde{D}$-core with the highest influenced expectation.

There are two potential greedy strategies. Given a connected $\tilde{D}$-core D, removing a vertex v from D results in a new connected $\tilde{D}$-core D'_v. The first greedy strategy, Greedy I, deletes the vertex v with the minimum influenced expectation: $v = \arg\min_{u \in V_D} Ie(u,S)$. The second greedy strategy, Greedy II, removes v to maximize the influenced expectation of D'_v: i.e., $v = \arg\max_{u \in V_D} Ie(D'_u, S)$, where $D'_u = D - \{u\}$.

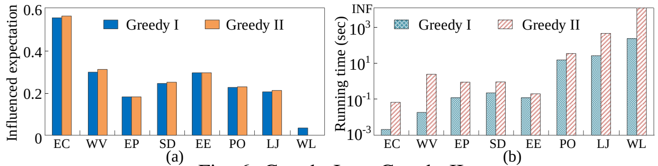

Fig. 6: Greedy I vs. Greedy II

To implement Greedy II, we must delete each vertex and check if D'_v yields the maximum influenced expectation. We compare these strategies on eight graphs and observe that (1) in Figure 6(a), the $\tilde{D}$-cores returned by Greedy I and Greedy II have similar influenced expectations, and (2) in Figure 6(b), Greedy I is up to 2 orders of magnitude faster than Greedy II. Therefore, we employ Greedy I in our algorithm. Next, we introduce a theorem to prune $\tilde{D}$-cores that cannot contain the $\tilde{D}$-core with the maximum influenced expectation.

Theorem 7. *Given two $\tilde{D}$-cores D_1 and D_2, and another $\tilde{D}$-core D_3 contained in D_2, i.e., $D_3 \subseteq D_2$, if $Ie(D_1, S) > \max_{v \in V_{D_2}} Ie(v, S)$, then $Ie(D_1, S) > Ie(D_3, S)$.*

Theorem 7 indicates that if the upper bound of $\tilde{D}$-core's influenced expectation (i.e., $\max_{v \in V_D} Ie(v, S)$) is lower than that of the currently found best community, then the corresponding $\tilde{D}$-core definitely does not contain the result community we are looking for and hence can be safely pruned.

Based on these considerations, we propose the algorithm GlobalSearch, with its pseudo code outlined in Algorithm 2. Initially, GlobalSearch performs initialization (Line 1) and computes the maximal D-core D of the input graph G (Line 2). Each connected component D_i of D with $|D_i| \geq \gamma$ is checked to determine if it may contain the $\tilde{D}$-core with the maximum influenced expectation and is added to the queue Q for further examination (Lines 3-5). If Q is not empty, GlobalSearch pops a $\tilde{D}$-core from Q and applies Greedy I to obtain a new $\tilde{D}$-core D (Lines 7-8). Similarly, it checks each connected component of D (Lines 9-12). When no $\tilde{D}$-core remains to be checked (i.e., $Q = \emptyset$), GlobalSearch returns the most influenced community (Line 13).

Time Complexity. The time complexity for computing the $\tilde{D}$-core and traversing all connected components in the $\tilde{D}$-core is $O(|V_G| + |E_G|)$. In the worst case, we may need $|V_G|$ iterations to traverse all $\tilde{D}$-cores and their connected components, resulting in a time complexity of $O(|V_G| \cdot (|V_G| + |E_G|)$. Thus, the time complexity of Algorithm 2 is $O(|V_G| \cdot (|V_G| + |E_G|)$.

B. Local Search Algorithm

The GlobalSearch algorithm finds the most influenced community using a top-down approach, iteratively removing vertices with the minimum influenced expectation from $\tilde{D}$-cores. In this subsection, we propose a new bottom-up approach to discover the most influenced community.

Peng et al [38] proposed a local algorithm for top-r influential community search using the *Avg* function. We extend this local algorithm to apply to our problem. Each time a vertex is added to the community, we evaluate whether the updated community still meets the size constraint γ and whether it contains a connected $\tilde{D}$-core. If both conditions are met, this connected $\tilde{D}$-core is returned as the result. The community with the largest influenced expectation is then selected as the MIC. However, this method is less efficient and often results in a community with suboptimal influenced expectation, as demonstrated by the experimental results in Section VII. To address this, we propose a new local algorithm, LocalSearch.

Algorithm 2 GlobalSearch

Input: a graph $G(V_G, E_G)$, two parameters k and l, a size constraint γ, the influenced expectation $Ie(v, S)$ for $\forall v \in V_G$
Output: the most influenced community MIC with $|MIC| \geq \gamma$

```
1:  MIC ← ∅; Queue Q ← ∅;
2:  Compute the maximal D-core D of G;
3:  for each connected component D_i of D with |D_i| ≥ γ do
4:      if Ie(D_i, S) ≥ Ie(MIC, S) then MIC ← D_i;
5:      if max_{v∈V_{D_i}} Ie(v, S) ≥ Ie(MIC, S) then Add D_i into Q;
6:  while Q ≠ ∅ do
7:      Pop a D̃-core D from Q; v ← arg min_{u∈V_D} Ie(u, S);
8:      Remove v from D; Maintain D by iteratively removing vertices that
        do not satisfy degree constraints of D̃-core;
9:      for each connected component D_i of D with |D_i| ≥ γ do
10:         if Ie(D_i, S) ≥ Ie(MIC, S) then MIC ← D_i;
11:         if max_{v∈V_{D_i}} Ie(v, S) ≥ Ie(MIC, S) then
12:             Add D_i into Q;
13: Return MIC.
```

The core idea behind our LocalSearch is to identify the *local most influenced community* for each node and ultimately return the one with the maximum influenced expectation. Here, the local most influenced community denotes the connected $\tilde{D}$-core that has at least γ size, contains a specific node, and has the maximal influenced expectation. Specifically, LocalSearch first computes the maximal D-core D of the given graph and sorts all nodes of D in descending order of their influenced expectations. Then, starting from the node v with the maximum influenced expectation, LocalSearch finds a new connected $\tilde{D}$-core $D' \subseteq D$ with the maximal influenced expectation containing v as the local most influenced community, denoted as MIC_v. After MIC_v is found, LocalSearch removes v from D, and repeats the process to find $\text{MIC}_{v'}$ for the next node v'. This continues until all nodes are processed. Finally, LocalSearch returns the local most influenced community with the maximum influenced expectation.

A key challenge for LocalSearch is efficiently computing the local most influenced community MIC_v for each node v. This involves gradually expanding v's neighbors. Specifically, MIC_v is initialized with v, and then the i-hop neighbors of v are added to MIC_v sequentially for $i = 1$ to $i = diam(G)$, where $diam(G)$ denotes the diameter of the graph G. Among neighbors with the same hop distance from v, those with higher influenced expectations are prioritized. After each addition, MIC_v is examined to determine if it contains a connected $\tilde{D}$-core that includes node v and meets the size constraint γ. If such a $\tilde{D}$-core exists, it is returned as MIC_v.

To enhance efficiency, we introduce several pruning strategies in LocalSearch to avoid unnecessary computations.

Pruning strategy 1. Assume nodes are processed in descending order of their influenced expectations. Let MIC_{v_i} represent the local most influenced community for node v_i. For the subsequent node v_{i+1}, if $Ie(\text{MIC}_{v_i}, S) > Ie(v_{i+1}, S)$, then we do not need to compute the local most influenced communities for nodes after v_i. This is because MIC_{v_i} can only be formed by vertex v_i and subsequent nodes having smaller influenced

Algorithm 3 LocalSearch

Input: a graph $G(V_G, E_G)$, two parameters k and l, a size constraint γ, the influenced expectation $Ie(v,S)$ for $\forall v \in V_G$
Output: the most influenced community MIC with $|MIC| \geq \gamma$
1: $MIC \leftarrow \emptyset$; Queue $Q \leftarrow \emptyset$;
2: Compute the maximal D-core D of G;
3: Sort all nodes v of D's connected components $D_i \subseteq D$ with $|D_i| \geq \gamma$ in descending order of $Ie(v,S)$ and add them into Q;
4: **while** $Q \neq \emptyset$ **do**
5: Pop a vertex v from Q;
6: **if** $Ie(v,S) < Ie(MIC,S)$ **then Break**; *//Pruning strategy 1*
7: **if** v is pruned **then Continue**;
8: $\text{MIC}_v \leftarrow$ **SearchLocalMIC** (v, D);
9: **if** $Ie(MIC_v,S) > Ie(MIC,S)$ **then** $MIC \leftarrow MIC_v$;
10: $D' \leftarrow$ Remove v from D and iteratively remove vertices that do not satisfy degree constraints of $\tilde{D}$-core;
11: **for** each node $v' \in V_D - V_{D'}$ **do** *// Pruning strategy 2(i)*
12: Mark v' as pruned.
13: **for** each connected component D'_i of D' **do**
14: **if** $|D'_i| < \gamma$ **then** *// Pruning strategy 2(ii)*
15: **for** each node $v' \in V_{D'_i}$ **do** Mark v' as pruned.
16: **Return** MIC.

expectations, i.e., $Ie(v_i,S) = \max_{v \in V_{\text{MIC}_{v_i}}} Ie(v,S)$. In other words, for any node v, it holds that $Ie(v,S) \geq Ie(\text{MIC}_v,S)$. If $Ie(\text{MIC}_{v_i},S) > Ie(v_{i+1},S)$, then $Ie(\text{MIC}_{v_i},S)$ will also be greater than $Ie(\text{MIC}_{v_j},S)$ for all $j \geq i+1$. Consequently, node v_{i+1} and those following it can be safely pruned.

Pruning strategy 2. After computing MIC_v, node v is removed from D. This removal may result in some vertices' in-degree and out-degree failing to meet the degree constraints of $\tilde{D}$-core. To address this, we can iteratively remove these vertices to obtain a new $\tilde{D}$-core $D' \subset D$. Specifically, (i) Vertices in $V_D - V_{D'}$ can be pruned, as there will be no $\tilde{D}$-core containing these vertices, implying their local most influenced communities are empty. (ii) For each connected component D'_i of D', if $|D'_i| < \gamma$, all vertices of D'_i can be pruned, since we only consider $\tilde{D}$-core of size at least γ.

Pruning strategy 3. Evaluating $\tilde{D}$-core can be computationally expensive each time a node is added to MIC_v. We propose the following rules to reduce unnecessary calculations: (i) After adding a node u to MIC_v, if u's in-degree or out-degree in MIC_v do not satisfy the degree constraints of $\tilde{D}$-core, we can skip the $\tilde{D}$-core examination and proceed to the next node. (ii) When peeling MIC_v to check whether MIC_v contains a $\tilde{D}$-core, if v is removed from MIC_v, the peeling process can be ended early. (iii) If MIC_v contains fewer than γ nodes, we can skip the $\tilde{D}$-core examination.

The pseudo-code for the LocalSearch algorithm is provided in Algorithm 3. The algorithm begins by computing the maximal D-core D of the graph G, sorting all nodes v within the connected components $D_i \subseteq D$ with $|D_i| \geq \gamma$ by descending influenced expectations $Ie(v,S)$, and enqueueing them into an empty queue Q (Lines 1-3). LocalSearch then processes the nodes as follows. It dequeues a vertex v from Q and checks whether to compute MIC_v (Lines 6-7). If the computation is warranted, it calculates MIC_v using the function SearchLocalMIC and updates MIC (Lines 8-9). It then removes v from D, maintains D by iteratively removing vertices that do not meet degree constraints of $\tilde{D}$-core, and computes a new $\tilde{D}$-core D'. Using both D and D', LocalSearch prunes vertices whose local most influenced communities cannot contribute to the final result, following Pruning Strategy 2 (Lines 10-15). This process continues until all vertices in Q are examined, after which it returns MIC (Line 16).

Algorithm 4 SearchLocalMIC

Input: v, D
Output: MIC_v
1: $D_v \leftarrow$ the connected component of D containing v;
2: **for** each node $u \in V_{D_v}$ **do** Mark u as unvisited;
3: $MIC_v \leftarrow \emptyset$; Queue $Q' \leftarrow \emptyset$; $G' \leftarrow \emptyset$;
4: Add v into Q;
5: **while** $Q \neq \emptyset$ **do**
6: Pop u from Q; Mark u as visited; $G' \leftarrow G' \oplus u$;
7: **if** $d^{in}_{G'}(u) \geq k \wedge d^{out}_{G'}(u) \geq l \wedge |V_{G'}| \geq \gamma$ **then**
8: $D'_v \leftarrow$ Compute the connected $\tilde{D}$-core of G' that contains v and has a size of at least γ;
9: **if** $D'_v \neq \emptyset$ **then** $MIC_v \leftarrow D'_v$; **Break**;
10: $N(u) \leftarrow$ all unvisited neighbors of u in D_v;
11: Sort all nodes w in $N(u)$ in descending order of $Ie(w,S)$;
12: **for** each node $w \in N(u)$ **do** Add w into Q; Mark w as visited;
13: **Return** MIC_v.

Algorithm 4 shows the pseudo-code of SearchLocalMIC. The function identifies the connected component D_v containing node v from the $\tilde{D}$-core D (Line 1) and marks all nodes in D_v as unvisited (Line 2). It initializes the $\tilde{D}$-core by adding node v to the queue Q (Line 4). Next, it dequeues a node u from Q, marks it as visited, and adds it to G' (Line 6). If u meets the degree constraints and $V_{G'}$ has at least γ nodes, it computes the $\tilde{D}$-core D'_v in G' that contains v and has a size of at least γ (Lines 7-8). If D'_v is non-empty, it is returned as the local most influenced community of v (Line 9). Otherwise, the function sorts all u's unvisited neighbors by descending influenced expectations and adds them to Q (Lines 10-12). The process continues until MIC_v is found or Q is empty.

Time Complexity. Following the complexity analysis of Algorithm 2, Algorithm 4 has a worst-case time complexity of $O(|L_v|(|V_G|+|E_G|))$. With ω nodes having lower influenced expectation than the MIC, Algorithm 3 computes the local most influenced community for $(|V_G|-\omega)$ nodes. Thus, the time complexity of Algorithm 3 is $O(|L_v|(|V_G|-\omega)(|V_G|+|E_G|))$.

VII. Experiments

In this section, we empirically evaluate our proposed algorithms. All implementations are done in C++ and executed on a Linux server with 3.70GHz CPU and 128GB of RAM.

Our experiments utilize eight real-world directed networks, detailed in Table I. The *WikiLink* is from Konect [73], while the others are available on SNAP [74]. For each network, we apply the *weighted-cascade* model [27] to compute the influence weight $w(u,v)$ for each edge, i.e., $w(u,v) = 1/|d^{in}_G(v)|$.

Following [75], we generate two types of seed node sets: *skewed* and *random*. The skewed seeds consist of the most influential nodes representing popular or influential users within the network. In contrast, the random seeds are sampled randomly from the network. Since the results from these two types of seed nodes are similar, we only present the results from the skewed seed set for brevity. Detailed results from the random seed set can be found in [25]. Our source code is available on https://github.com/ZJU-DAILY/MICS.

A. Performance of the Predictive Models

In our first set of experiments, we evaluate the performance of the predictive models used in L-InfExp algorithm. We

TABLE I: Dataset Statistics

Dataset	n	m	d_{avg}	k_{max}	l_{max}
EmailCore (EC)	1,005	25,571	49.6	27	26
WikiVote (WV)	7,115	103,689	14.57	19	15
Epinions (EP)	75,879	508,837	6.7	40	42
Slashdot (SD)	82,168	948,464	11.54	54	9
EmailEuall (EE)	265,214	420,045	1.58	28	28
Pokec (PO)	1,632,803	30,622,564	18.75	32	31
LiveJournal (LJ)	4,847,571	68,993,773	14.13	252	253
WikiLink (WL)	13,593,032	437,217,424	64.33	1086	1086

assess three models: Random Forest (RF) [69], Decision Tree (DT) [71], and k-Nearest Neighbor (KNN) [70].

We employ Random Forest in L-InfExp due to its superior predictive performance, as demonstrated in Exp-1 and Exp-2. We set the default sample size to 20 and use the following hyperparameters for RF: *NE*=100, *MD*=None, *MSL*=1, and *MSS*=2. Specifically, *NE* refers to the number of decision trees; *MD* indicates the maximum depth of each decision tree; *MSL* and *MSS* represent the minimum number of samples required to split a leaf node and an internal node, respectively.

Exp-1: Spearman coefficient analysis. We conducted a Spearman coefficient analysis experiment on six datasets. As shown in Table II, the Spearman coefficients for all datasets across the three models are all very close to 1. This indicates that the rankings of influenced expectations for L-InfExp and S-InfExp are nearly identical, suggesting a strong alignment between the results of both methods. Additionally, we observed that RF model achieves the best predictive accuracy on most datasets, showing the smallest disparity between predicted and actual influenced expectations.

Exp-2: Performance of predictive models. In this experiment, we compare RF, DT, and KNN. We generate 20 seed node sets and compute the influenced expectations for each set. Of these, 15 sets are used for training and the remaining 5 for testing. For each model, we report both *training time* (T-time) and *prediction time* (P-time), as well as *predictive accuracy*. For MSE, RMSE, and MAE, lower values indicate better performance. For R-squared, higher values are preferred. The results, summarized in Table III, show that RF delivers the best predictive accuracy among the three models, with the smallest disparity between predicted and actual influenced expectations. Therefore, we employ RF in the L-InfExp algorithm due to its superior predictive accuracy.

Exp-3: Sensitivity analysis of RF model. We conduct a sensitivity analysis of RF on *Epinions*. We randomly select 50% of the samples for training and the remaining 50% for testing. Results in Table IV show that increasing MSL and MSS reduces training time, as larger values require fewer split, thereby reducing tree depth and model complexity and lowering the computational cost of finding optimal splits. However, prediction time remains relatively stable, since the number of trees and their traversal paths do not change significantly. Higher MSL and MSS lower prediction performance due to model simplification. Increasing NE increases both training and prediction times, while MD and NE have little effect on accuracy. Lower MSL and MSS improve performance. Based on these findings, the default hyperparameters are set as: MD

TABLE II: Spearman Coefficient Analysis

Model \ Dataset	EC	WV	EP	SD	EE	PO
Random Forest (RF)	**0.9688**	**0.9967**	0.9937	**0.9798**	0.9983	**0.9914**
Decision Tree (DT)	0.8506	0.9953	0.9933	0.9178	0.9985	0.9240
k-Nearest-Neighbor (KNN)	0.9678	0.9964	**0.9942**	0.9744	**0.9991**	0.9815

=None, MSL $= 1$, MSS $= 2$, and NE $= 100$.

B. Efficiency Evaluation

In this set of experiments, we evaluate the efficiency of our proposed algorithms. Due to space constraint and similar results, we present results for the *EmailEuall* and *Wiki-Link* in this paper. Results for other datasets can be found in [25].

Algorithms. To our best knowledge, this is the first work studying the Most Influenced Community search in large social graphs. Hence, for comparative methods, we extend two widely-used existing algorithms: Monte-Carlo simulation (MCS) [27], designed for influence maximization, and local search [38], developed for identifying the top-r influential communities, to address our problem. Therefore, we compare six methods listed as follows:

For **Phase I**-Influenced expectation computation:

- **S-InfExp**: our proposed sampling-based algorithm.
- **L-InfExp**: our proposed learning-based algorithm.
- **M-InfExp**: an extended MCS-based algorithm [27].

For **Phase II**-MIC search:

- **GlobalSearch**: our proposed global search algorithm.
- **LocalSearch**: our proposed local search algorithm.
- **NeiborSearch**: a method extended from the local search algorithm proposed in [38].

Parameters. We test parameters including D-core integers k and l, seed set size $|S|$, community size threshold γ, graph size $|V_G|$, and influence propagation instances $|\mathcal{I}|$. Each experiment varies one parameter while keeping others at default values. For small datasets such as *EmailCore*, *WikiVote*, *Epinions*, *Slashdot*, and *EmailEuall*, we set $|S| = 50$; for large datasets like *Pokec*, *LiveJournal*, and *WikiLink*, $|S| = 500$. Default values for $|\mathcal{I}|$ and γ are 2000 and 100, respectively. We terminate an algorithm if it cannot finish in 24 hours.

Exp-4: Effect of $|S|$. We analyze how the number of seed nodes $|S|$ affects running time. Results are shown in Figures 7(a) and 8(a). We observe that the running times of M-InfExp and S-InfExp increase with $|S|$, as they need to generate more influence propagation instances, resulting in higher running time. In addition, it can be seen that S-InfExp runs faster than M-InfExp because S-InfExp skips certain nodes when sampling influence propagation instances, thereby improving sampling efficiency. L-InfExp, on the other hand, maintains a relatively stable and lower running time. Moreover, the running times of NeiborSearch, GlobalSearch, and LocalSearch remain relatively stable with $|S|$ since this parameter mainly influences the computation of influenced expectations. Notably, LocalSearch is significantly faster than GlobalSearch and NeiborSearch across all settings.

Exp-5: Effect of γ. We investigate the impact of the size constraint γ on algorithm performance. Figures 7(b) and 8(b) show the results. We can observe that increasing γ has little effect on running time across all algorithms for influenced

TABLE III: Performance of Predicting Models

Model	Pokec						Livejournal						WikiLink					
	T-time	P-time	MSE	RMSE	MAE	R-Squared	T-time	P-time	MSE	RMSE	MAE	R-Squared	T-time	P-time	MSE	RMSE	MAE	R-Squared
RF	701.65s	0.0964s	**6.29E-05**	**0.0079**	**0.0031**	**0.9909**	2241.8s	0.5089s	**5.26E-05**	**0.0072**	**0.0023**	**0.9891**	6309.8s	1.4454s	**6.47E-05**	**0.0080**	**0.0018**	**0.9919**
DT	21.906s	**0.0024s**	0.0005	0.0229	0.0093	0.9238	70.219s	**0.0119s**	0.0003	0.0198	0.0064	0.9186	200.98s	**0.0393s**	0.0004	0.0209	0.0044	0.9452
KNN	**0.0433s**	0.0535s	0.0002	0.0139	0.0052	0.9720	**0.1142s**	0.1664s	0.0001	0.0122	0.0036	0.9692	**0.1715s**	0.4785s	0.0002	0.0150	0.0027	0.9716

TABLE IV: Sensitivity Analysis of Random Forest model (Dataset: Epinions)

MD	T-time	P-time	MSE	R-Squard	MSL	T-time	P-time	MSE	R-Squard	MSS	T-time	P-time	MSE	R-Squard	NE	T-time	P-time	MSE	R-Squard
None	4.5851	0.009	0.0034	0.7594	**1**	4.5986	0.0091	0.0034	0.7594	**2**	4.7158	0.0091	0.0034	0.7594	**50**	2.3972	0.0048	0.0034	0.7618
5	4.5882	0.009	0.0034	0.7594	**2**	2.2397	0.01	0.0049	0.6795	**5**	2.7278	0.009	0.0051	0.6828	**100**	4.7405	0.0091	0.0034	0.7594
10	4.5853	0.009	0.0035	0.7594	**4**	0.6106	0.009	0.0094	0.3915	**8**	0.7821	0.009	0.0094	0.3974	**150**	7.0352	0.0133	0.0033	0.7465
20	4.5896	0.009	0.0034	0.7594	**6**	0.449	0.009	0.0104	0.3307	**10**	0.4473	0.009	0.0104	0.3307	**200**	9.2079	0.0175	0.0034	0.7478

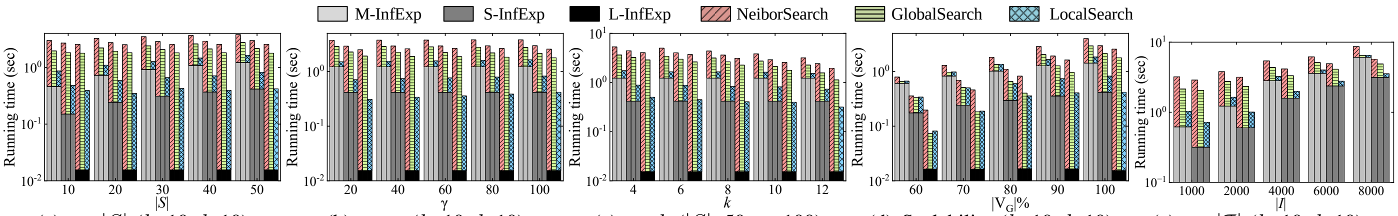

(a) vs. $|S|$ (k=10, l=10) (b) vs. γ (k=10, l=10) (c) vs. k ($|S|$=50, γ=100) (d) Scalability (k=10, l=10) (e) vs. $|\mathcal{I}|$ (k=10, l=10)

Fig. 7: Running time on EmailEuall

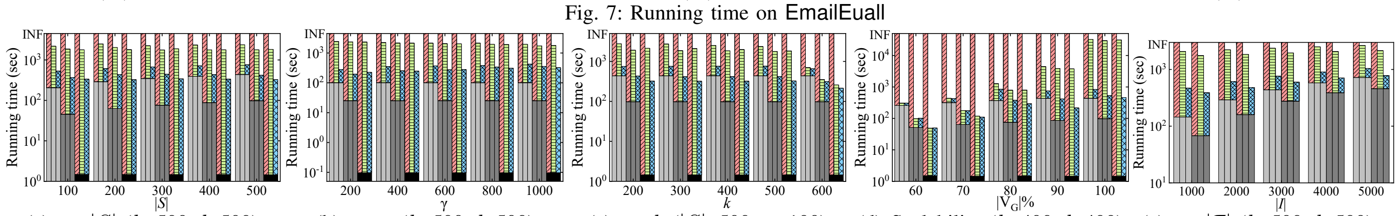

(a) vs. $|S|$ (k=500, l=500) (b) vs. γ (k=500, l=500) (c) vs. k ($|S|$=500, γ=100) (d) Scalability (k=400, l=400) (e) vs. $|\mathcal{I}|$ (k=500, l=500)

Fig. 8: Running time on WikiLink

expectation computation. Moreover, the running time of GlobalSearch decreases as γ increases. This is because a larger γ results in the generation of new connected components that are less likely to meet the size condition, which in turn reduces the number of communities that need to be examined. However, both NeiborSearch and LocalSearch show a slight increase in running time with larger γ. This is due to the fact that, more vertices need to be inserted to search for the local most influenced community that meets the larger size condition, resulting in increased time required to compute the D-core and traverse all connected components.

Exp-6: Effect of k and l. We evaluate the effects of parameters k and l on algorithm performance. Figures 7(c) and 8(c) present the results for k. The results for l, which are similar to the results for k, are reported in our technical report [25]. As k (or l) increases, the running time for NeiborSearch, GlobalSearch, and LocalSearch decreases because a larger k results in a smaller D-core, reducing the number of nodes that need to be processed. The running times of M-InfExp, S-InfExp, and L-InfExp remain unchanged as k and l only impact the community search, not influenced expectations computation.

Exp-7: Scalability. We assess the scalability of our algorithms by varying the graph size. To this end, we randomly select a certain number of nodes from the graph to form the induced subgraph and test the running time of all algorithms. Figures 7(d) and 8(d) illustrate that the running times of all algorithms, except for L-InfExp, increase as the graph size grows. This is because NeiborSearch, GlobalSearch, and LocalSearch require more time to identify communities in larger graphs. For M-InfExp and S-InfExp, the increased running time is mainly due to the larger size of influence propagation instances. The running time of L-InfExp remains stable, as the efficiency of this learning based algorithm is not sensitive to the graph size.

Exp-8: Effect of $|\mathcal{I}|$. We evaluate the impact of the number of influence propagation instances $|\mathcal{I}|$ on algorithm efficiency. The results are shown in Figures 7(e) and 8(e). We observe that the running times of M-InfExp and S-InfExp increase with $|\mathcal{I}|$, reflecting their time complexity. In addition, S-InfExp runs faster than M-InfExp across all settings. In contrast, NeiborSearch, GlobalSearch, and LocalSearch show stable running times as $|\mathcal{I}|$ varies, since $|\mathcal{I}|$ mainly affects the computation of influenced expectations.

C. Effectiveness Evaluation

In this set of experiments, we evaluate the quality of returned communities.

Exp-9: MIC under different aggregate functions. We evaluate the influenced expectation of the most influenced community (MIC) using three aggregate functions: *avg*, *min*, and *percentile*. We extend our GlobalSearch and LocalSearch to find the community defined under the *min* and *50-th percentile* aggregate function. For comparisons, we also report the influenced expectations for the entire graph and the maximal D-core. We set all parameters to their default values. The results are summarized in Table V. From Table V, we make the following observations. **(1)** The MIC identified by the GlobalSearch algorithm has a higher influenced expectation compared to the MIC found by LocalSearch and NeiborSearch. **(2)** The influenced expectation of the MIC computed by the L-InfExp algorithm is very close to that of the MIC calculated by S-InfExp, indicating the prediction accuracy of the L-InfExp algorithm. **(3)** The expected influence of the MIC computed by the M-InfExp algorithm is slightly higher than that of S-InfExp. **(4)** The influenced expectation of the MIC is significantly

TABLE V: Influenced Expectations Comparison

Dataset	Avg Function															Min Function						50-th Percentile Function					
	MIC									Original Graph			Maximal D-core			MIC						MIC					
	M+G	M+L	M+N	S+G	S+L	S+N	L+G	L+L	L+N	M-INF	S-INF	L-INF	M-INF	S-INF	L-INF	M+G	M+L	S+G	S+L	L+G	L+L	M+G	M+L	S+G	S+L	L+G	L+L
EC ($k=10$, $l=10$, $\gamma=20$)	0.9748	0.9212	0.9718	<u>0.9749</u>	0.9312	0.9742	0.9348	0.8753	0.9348	0.4409	0.4122	0.4108	0.4588	0.4317	0.4300	0.4963	0.4963	0.4970	0.4970	0.5220	0.5220	**1.0000**	**1.0000**	**1.0000**	**1.0000**	0.9560	0.9560
WV ($k=5$, $l=5$, $\gamma=20$)	0.5738	0.4526	0.5738	0.5628	0.6019	0.5370	<u>0.6044</u>	**0.6332**	0.4566	0.0833	0.0804	0.0804	0.2762	0.2699	0.2702	0.2727	0.2727	0.2720	0.2720	0.2700	0.2700	0.3077	0.2872	0.3030	0.3075	0.3880	0.6355
EP ($k=20$, $l=20$, $\gamma=20$)	**0.2516**	<u>0.2438</u>	0.2412	0.2312	0.2175	0.2176	0.2246	0.2122	0.2173	0.1572	0.1410	0.1387	0.2152	0.1882	0.1836	0.1997	0.1997	0.1760	0.1760	0.1720	0.1720	0.2113	0.2080	0.1870	0.1850	0.1820	0.1800
SD ($k=40$, $l=5$, $\gamma=20$)	**0.2808**	<u>0.2770</u>	0.2721	0.2639	0.2640	0.2639	0.2704	0.2763	0.2621	0.2100	0.1813	0.1829	0.2621	0.2445	0.2472	0.2070	0.2070	0.1890	0.1890	0.1920	0.1920	0.2237	0.2237	0.2090	0.2090	0.2115	0.2120
EE ($k=10$, $l=10$, $\gamma=20$)	**0.7564**	0.6781	0.7534	0.7344	0.7239	0.7344	<u>0.7480</u>	0.6641	0.7460	0.0651	0.0618	0.0613	0.1822	0.1561	0.1544	0.1690	0.1690	0.1350	0.1350	0.1520	0.1520	0.3096	0.3083	0.3071	0.3064	0.3041	0.3055
PO ($k=23$, $l=23$, $\gamma=100$)	**0.2422**	<u>0.2393</u>	0.2322	0.2364	0.2186	0.2364	0.2353	0.2187	0.2353	0.0954	0.0720	0.0713	0.1045	0.0871	0.0869	0.1723	0.1723	0.1590	0.1590	0.1600	0.1600	0.1935	0.1923	0.1840	0.1780	0.1810	0.1780
LJ ($k=75$, $l=75$, $\gamma=100$)	**0.2547**	<u>0.2534</u>	0.2530	0.2465	0.2460	0.2465	0.2412	0.2407	0.2412	0.0487	0.0375	0.0364	0.0188	0.0174	0.0169	0.2017	0.2017	0.1920	0.1920	0.1910	0.1910	0.2280	0.2280	0.2190	0.2185	0.2160	0.2160
WL ($k=500$, $l=500$, $\gamma=100$)	<u>0.0508</u>	0.0507	0.0501	0.0399	0.0397	0.0399	0.0389	0.0388	0.0389	0.0350	0.0299	0.0293	0.0104	0.0089	0.0088	0.0092	0.0092	0.0050	0.0050	0.0060	0.0060	**0.0572**	**0.0572**	0.0390	0.0390	0.0390	0.0390

* **M**/**S**/**L**+**G**/**L**/**N**: **M**-InfExp/**S**-InfExp/**L**-InfExp+**G**lobalSearch/**L**ocalSearch/**N**eiborSearch.

TABLE VI: Comparison of MIC Search Methods on EmailCore

Parameters	$k=25, l=25, \gamma=115$			$k=25, l=25, \underline{\gamma=114}$			$k=25, l=25, \underline{\gamma=113}$			$k=25, l=25, \underline{\gamma=112}$			$\underline{k=24}, l=25, \gamma=115$			$k=25, \underline{l=24}, \gamma=115$		
MIC search method	**Enum.**	**Global.**	**Local.**	**Enum.**	**Global.**	**Local.**	**Enum.**	**Global.**	**Local.**	**Enum.**	**Global.**	**Local**	**Enum.**	**Global.**	**Local.**	**Enum.**	**Global.**	**Local.**
Influenced expectation	0.5509	0.5489	0.5459	0.5526	0.5524	0.5459	0.5542	0.5541	0.5459	0.5559	0.5559	0.5483	0.5510	0.5509	0.5445	/	0.5485	0.5476
Running time (sec)	116.1	0.0037	0.0056	990.9	0.0018	0.0029	7167.8	0.0018	0.0031	66042.6	0.0023	0.0032	2651.6	0.0018	0.0031	> 7 days	0.0039	0.0083
Number of $\tilde{D}$-core	6,776	/	/	48,484	/	/	237,977	/	/	880,064	/	/	156,506	/	/	/	/	/

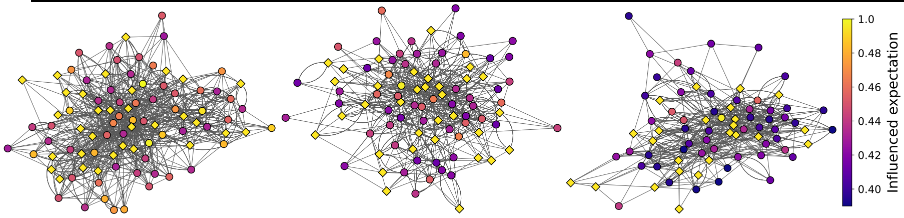

(a) MIC-I (D-core) (b) MIC-II (k-core) (c) MIC-III (k-truss)

Fig. 9: Case studies on EmailCore (seed node: diamond, other node: circle)

TABLE VII: Comparison of InfExp Methods

Dataset	R-InfExp		S-InfExp		L-InfExp	
	Global.	Local.	Global.	Local.	Global.	Local.
EC ($k=10$, $l=10$)	0.5859	0.4751	0.6506	0.5732	0.6433	0.5734
EP ($k=20$, $l=20$)	0.1018	0.1002	0.2312	0.2175	0.2246	0.2122
PO ($k=23$, $l=23$)	0.1014	0.1100	0.2364	0.2286	0.2353	0.2287
LJ ($k=75$, $l=75$)	0.0648	0.0671	0.2465	0.2460	0.2412	0.2407

greater than that of the whole graph and the maximal D-core, suggesting that nodes in the MIC are more likely to be influenced by the seed nodes. **(5)** The influenced expectation of the MIC found by the NeiborSearch method is lower than that found using our methods, demonstrating the superiority of our proposed algorithms. **(6)** The influenced expectation of the MIC under function *min* is lower than that of the MIC under function *avg*, consistent with our expectation. **(7)** Except for the EC and WL datasets, the community identified by the *avg* function achieves a higher influenced expectation than *50-th percentile*. Overall, the community identified by function *avg* and our proposed algorithms demonstrate the best quality.

Exp-10: S-InfExp & L-InfExp V.S. R-InfExp. In this experiment, we compare our algorithms S-InfExp and L-InfExp with RMPP-based [59] solution, denoted by R-InfExp. Table VII shows the influenced expectations of the communities. We can observe that the influenced expectation of the MIC computed by R-InfExp is significantly smaller than that of S-InfExp and L-InfExp, while the influenced expectation of the MIC computed by L-InfExp is very close to that of S-InfExp.

Exp-11: GlobalSearch & LocalSearch V.S. Enumerate. In this experiment, we compare our proposed algorithms GlobalSearch and LocalSearch with an alternative solution called Enumerate. Specifically, Enumerate enumerates all $\tilde{D}$-cores of D to identify the one with the maximum influenced expectation. Table VI shows the results. We can observe that the communities returned by GlobalSearch, LocalSearch, and Enumerate have the similar influenced expectations. However, GlobalSearch and LocalSearch are 5-10 orders of magnitude faster than Enumerate. Overall, both GlobalSearch and LocalSearch significantly outperform Enumerate.

Exp-12: Case study. We conduct a case study using email communication network EmailCore. We select 50 senior researchers as seed users who share academic findings with other researchers via email and set $k = l = 25$ and $\gamma = 100$. Figure 9 shows the results. Specifically, D-core, k-core, and k-truss return the most influenced communities MIC-I, MIC-II, and MIC-III, respectively. The communities represent densely connected scholars who are influenced by authoritative scholars (i.e., the seed nodes). We can observe that MIC-I exhibits a greater density than MIC-II, indicating that scholars in MIC-I are more densely connected. In addition, MIC-I is larger than MIC-III, showing that MIC-III miss some important scholars due to not considering the edge directions. Furthermore, nodes within the MIC-I have higher influenced expectations than those in MIC-II and MIC-III, resulting in an overall higher influenced expectation of MIC-I. These results underscore the superiority of the D-core.

VIII. Conclusion

In this paper, we introduce the most influenced community search problem. First, we propose two algorithms S-InfExp and L-InfExp to compute the influenced expectation of each node using sampling and learning techniques, respectively. To identify the most influenced community based on these expectations, we further design algorithms GlobalSearch and LocalSearch, which follow top-down and bottom-up manners, respectively. Extensive experiments show that our algorithms are effective, efficient, and scalable. In future work, we plan to employ reusing sampled instances to further reduce the computational cost of S-InfExp and use the graph structure to improve the prediction accuracy of L-InfExp.

Acknowledgements

This work was supported in part by the NSFC under Grants No. (62302444, 62025206, and U23A20296), and Zhejiang Province's "Lingyan" R&D Project under Grant No 2024C01259. Qing Liu is the corresponding author of the work.

References

[1] F. Zhou, X. Xu, G. Trajcevski, and K. Zhang, "A survey of information cascade analysis: Models, predictions, and recent advances," *ACM Computing Surveys (CSUR)*, vol. 54, no. 2, pp. 1–36, 2021.

[2] Y. Li, J. Fan, Y. Wang, and K.-L. Tan, "Influence maximization on social graphs: A survey," *IEEE Transactions on Knowledge and Data Engineering*, vol. 30, no. 10, pp. 1852–1872, 2018.

[3] R. Bian, Y. S. Koh, G. Dobbie, and A. Divoli, "Identifying top-k nodes in social networks: a survey," *ACM Computing Surveys (CSUR)*, vol. 52, no. 1, pp. 1–33, 2019.

[4] Y. Yang and J. Pei, "Influence analysis in evolving networks: A survey," *IEEE Transactions on Knowledge and Data Engineering*, vol. 33, no. 3, pp. 1045–1063, 2019.

[5] H. Li, C. Xia, T. Wang, S. Wen, C. Chen, and Y. Xiang, "Capturing dynamics of information diffusion in sns: A survey of methodology and techniques," *ACM Computing Surveys (CSUR)*, vol. 55, no. 1, pp. 1–51, 2021.

[6] F. Zhou, X. Xu, K. Zhang, G. Trajcevski, and T. Zhong, "Variational information diffusion for probabilistic cascades prediction," in *IEEE INFOCOM 2020-IEEE conference on computer communications*. IEEE, 2020, pp. 1618–1627.

[7] T. R. Zaman, R. Herbrich, J. Van Gael, and D. Stern, "Predicting information spreading in twitter," in *Workshop on computational social science and the wisdom of crowds, nips*, vol. 104, no. 45. Citeseer, 2010, pp. 17 599–601.

[8] B. Zhang, Z. Qian, and S. Lu, "Structure pattern analysis and cascade prediction in social networks," in *Machine Learning and Knowledge Discovery in Databases: European Conference, ECML PKDD*. Springer, 2016, pp. 524–539.

[9] S. Huang, Z. Bao, J. S. Culpepper, and B. Zhang, "Finding temporal influential users over evolving social networks," in *2019 IEEE 35th international conference on data engineering (ICDE)*. IEEE, 2019, pp. 398–409.

[10] J. Zhao, S. Shang, P. Wang, J. C. Lui, and X. Zhang, "Tracking influential nodes in time-decaying dynamic interaction networks," in *2019 IEEE 35th International Conference on Data Engineering (ICDE)*. IEEE, 2019, pp. 1106–1117.

[11] Y. Zhu, J. Tang, and X. Tang, "Pricing influential nodes in online social networks," *Proceedings of the VLDB Endowment*, vol. 13, no. 10, pp. 1614–1627, 2020.

[12] Y. Wang, G. Cong, G. Song, and K. Xie, "Community-based greedy algorithm for mining top-k influential nodes in mobile social networks," in *Proceedings of the 16th ACM SIGKDD international conference on Knowledge discovery and data mining*, 2010, pp. 1039–1048.

[13] F. Riquelme and P. González-Cantergiani, "Measuring user influence on twitter: A survey," *Information processing & management*, vol. 52, no. 5, pp. 949–975, 2016.

[14] N. Hafiene, W. Karoui, and L. B. Romdhane, "Influential nodes detection in dynamic social networks: A survey," *Expert Systems with Applications*, vol. 159, p. 113642, 2020.

[15] Q. Guo, C. Feng, F. Zhang, and S. Wang, "Efficient algorithm for budgeted adaptive influence maximization: An incremental rr-set update approach," *Proceedings of the ACM on Management of Data*, vol. 1, no. 3, pp. 1–26, 2023.

[16] C. Borgs, M. Brautbar, J. Chayes, and B. Lucier, "Maximizing social influence in nearly optimal time," in *Proceedings of the twenty-fifth annual ACM-SIAM symposium on Discrete algorithms*. SIAM, 2014, pp. 946–957.

[17] Y. Tang, X. Xiao, and Y. Shi, "Influence maximization: Near-optimal time complexity meets practical efficiency," in *Proceedings of the 2014 ACM SIGMOD International Conference on Management of Data*, 2014, pp. 75–86.

[18] Y. Tang, Y. Shi, and X. Xiao, "Influence maximization in near-linear time: A martingale approach," in *Proceedings of the 2015 ACM SIGMOD International Conference on Management of Data*, 2015, pp. 1539–1554.

[19] J. Tang, X. Tang, X. Xiao, and J. Yuan, "Online processing algorithms for influence maximization," in *Proceedings of the 2018 ACM SIGMOD International Conference on Management of Data*, 2018, pp. 991–1005.

[20] Q. Guo, S. Wang, Z. Wei, and M. Chen, "Influence maximization revisited: Efficient reverse reachable set generation with bound tightened," in *Proceedings of the 2020 ACM SIGMOD International Conference on Management of Data*, 2020, pp. 2167–2181.

[21] SBDC, "Why target marketing is important and how to do it." 2024. [Online]. Available: https://georgiasbdc.org/why-target-marketing-is-important-and-how-to-do-it/

[22] X. Yao, X. Han, Y. Gu, C. Gu, and H. Huang, "Influence spread in location-based social network: An efficient algorithm of epidemic controlling," *IEEE Transactions on Computational Social Systems*, vol. 9, no. 4, pp. 1132–1143, 2021.

[23] A. Goyal, F. Bonchi, and L. V. Lakshmanan, "Learning influence probabilities in social networks," in *Proceedings of the third ACM international conference on Web search and data mining*, 2010, pp. 241–250.

[24] D. J. Watts, J. Peretti, and M. Frumin, *Viral marketing for the real world*. Harvard Business School Pub. Boston, 2007.

[25] X. Chang, Q. Liu, Y. Gao, B. Zheng, Y. Cai, and Q. Li, "The most influenced community search on social networks," 2024. [Online]. Available: https://github.com/ZJU-DAILY/MICS

[26] C. Giatsidis, D. M. Thilikos, and M. Vazirgiannis, "D-cores: measuring collaboration of directed graphs based on degeneracy," *Knowledge and information systems*, vol. 35, no. 2, pp. 311–343, 2013.

[27] D. Kempe, J. Kleinberg, and É. Tardos, "Maximizing the spread of influence through a social network," in *Proceedings of the ninth ACM SIGKDD international conference on Knowledge discovery and data mining*, 2003, pp. 137–146.

[28] HubSpot, "The 2025 state of marketing & trends report: Data from 1700+ global marketers." 2025. [Online]. Available: https://www.overleaf.com/project/67949fe6f66c9204370136d3

[29] J. Brown, A. J. Broderick, and N. Lee, "Word of mouth communication within online communities: Conceptualizing the online social network," *Journal of interactive marketing*, vol. 21, no. 3, pp. 2–20, 2007.

[30] R. M. Christley, G. Pinchbeck, R. G. Bowers, D. Clancy, N. P. French, R. Bennett, and J. Turner, "Infection in social networks: using network analysis to identify high-risk individuals," *American journal of epidemiology*, vol. 162, no. 10, pp. 1024–1031, 2005.

[31] K. Bringmann and K. Panagiotou, "Efficient sampling methods for discrete distributions," *Algorithmica*, vol. 79, pp. 484–508, 2017.

[32] S. Chen, R. Wei, D. Popova, and A. Thomo, "Efficient computation of importance based communities in web-scale networks using a single machine," in *Proceedings of the 25th ACM International on Conference on Information and Knowledge Management*, 2016, pp. 1553–1562.

[33] R.-H. Li, L. Qin, J. X. Yu, and R. Mao, "Finding influential communities in massive networks," *The VLDB Journal*, vol. 26, pp. 751–776, 2017.

[34] W. Luo, X. Zhou, J. Yang, P. Peng, G. Xiao, and Y. Gao, "Efficient approaches to top-r influential community search," *IEEE Internet of Things Journal*, vol. 8, no. 16, pp. 12 650–12 657, 2020.

[35] Y. Wu, J. Zhao, R. Sun, C. Chen, and X. Wang, "Efficient personalized influential community search in large networks," *Data Science and Engineering*, vol. 6, no. 3, pp. 310–322, 2021.

[36] R.-H. Li, L. Qin, J. X. Yu, and R. Mao, "Influential community search in large networks," *Proceedings of the VLDB Endowment*, vol. 8, no. 5, pp. 509–520, 2015.

[37] R.-H. Li, L. Qin, F. Ye, J. X. Yu, X. Xiao, N. Xiao, and Z. Zheng, "Skyline community search in multi-valued networks," in *Proceedings of the 2018 International Conference on Management of Data*, 2018, pp. 457–472.

[38] Y. Peng, S. Bian, R. Li, S. Wang, and J. X. Yu, "Finding top-r influential communities under aggregation functions," in *2022 IEEE 38th International Conference on Data Engineering (ICDE)*. IEEE, 2022, pp. 1941–1954.

[39] Y. Zhou, Y. Fang, W. Luo, and Y. Ye, "Influential community search over large heterogeneous information networks," *Proceedings of the VLDB Endowment*, vol. 16, no. 8, pp. 2047–2060, 2023.

[40] F. Bi, L. Chang, X. Lin, and W. Zhang, "An optimal and progressive approach to online search of top-k influential communities," *Proceedings of the VLDB Endowment*, vol. 11, no. 9, 2018.

[41] Y. Fang, X. Huang, L. Qin, Y. Zhang, W. Zhang, R. Cheng, and X. Lin, "A survey of community search over big graphs," *The VLDB Journal*, vol. 29, pp. 353–392, 2020.

[42] Q. Liu, M. Zhao, X. Huang, J. Xu, and Y. Gao, "Truss-based community search over large directed graphs," in *Proceedings of the 2020 ACM SIGMOD International Conference on Management of Data*, 2020, pp. 2183–2197.

[43] X. Liao, Q. Liu, J. Jiang, X. Huang, J. Xu, and B. Choi, "Distributed d-core decomposition over large directed graphs," *Proceedings of the VLDB Endowment*, vol. 15, no. 8, pp. 1546–1558, 2022.

[44] X. Huang and L. V. Lakshmanan, "Attribute-driven community search," *Proceedings of the VLDB Endowment*, vol. 10, no. 9, pp. 949–960, 2017.

[45] L. Chen, C. Liu, R. Zhou, J. Li, X. Yang, and B. Wang, "Maximum co-located community search in large scale social networks," *Proceedings of the VLDB Endowment*, vol. 11, no. 10, pp. 1233–1246, 2018.

[46] Q. Liu, Y. Zhu, M. Zhao, X. Huang, J. Xu, and Y. Gao, "Vac: vertex-centric attributed community search," in *2020 IEEE 36th International Conference on Data Engineering (ICDE)*. IEEE, 2020, pp. 937–948.

[47] Y. Fang, Y. Yang, W. Zhang, X. Lin, and X. Cao, "Effective and efficient community search over large heterogeneous information networks," *Proceedings of the VLDB Endowment*, vol. 13, no. 6, pp. 854–867, 2020.

[48] Y. Jiang, Y. Fang, C. Ma, X. Cao, and C. Li, "Effective community search over large star-schema heterogeneous information networks," *Proceedings of the VLDB Endowment*, vol. 15, no. 11, pp. 2307–2320, 2022.

[49] J. Wang, K. Wang, X. Lin, W. Zhang, and Y. Zhang, "Efficient unsupervised community search with pre-trained graph transformer," *Proceedings of the VLDB Endowment*, vol. 17, no. 9, pp. 2227–2240, 2024.

[50] Y. Jiang, Y. Rong, H. Cheng, X. Huang, K. Zhao, and J. Huang, "Query driven-graph neural networks for community search: from non-attributed, attributed, to interactive attributed," *Proceedings of the VLDB Endowment*, vol. 15, no. 6, pp. 1243–1255, 2022.

[51] M. Girvan and M. E. Newman, "Community structure in social and biological networks," *Proceedings of the national academy of sciences*, vol. 99, no. 12, pp. 7821–7826, 2002.

[52] J. Li, H. Zhang, Z. Han, Y. Rong, H. Cheng, and J. Huang, "Adversarial attack on community detection by hiding individuals," in *Proceedings of The Web Conference 2020*, 2020, pp. 917–927.

[53] X. Jian, Y. Wang, and L. Chen, "Effective and efficient relational community detection and search in large dynamic heterogeneous information networks," *Proceedings of the VLDB Endowment*, vol. 13, no. 10, pp. 1723–1736, 2020.

[54] Z. Xu, Y. Ke, Y. Wang, H. Cheng, and J. Cheng, "A model-based approach to attributed graph clustering," in *Proceedings of the 2012 ACM SIGMOD international conference on management of data*, 2012, pp. 505–516.

[55] A. Conte, T. De Matteis, D. De Sensi, R. Grossi, A. Marino, and L. Versari, "D2k: scalable community detection in massive networks via small-diameter k-plexes," in *Proceedings of the 24th ACM SIGKDD International Conference on Knowledge Discovery & Data Mining*, 2018, pp. 1272–1281.

[56] N. Veldt, D. F. Gleich, and A. Wirth, "A correlation clustering framework for community detection," in *Proceedings of the 2018 World Wide Web Conference*, 2018, pp. 439–448.

[57] X. Chang, X. Ke, L. Chen, C. Ge, Z. Wei, and Y. Gao, "Host profit maximization: Leveraging performance incentives and user flexibility," *Proceedings of the VLDB Endowment*, vol. 17, no. 1, pp. 51–64, 2023.

[58] Z. Liang, Y. Yang, X. Ke, X. Xiao, and Y. Gao, "A benchmark study of deep-rl methods for maximum coverage problems over graphs," *Proceedings of the VLDB Endowment*, vol. 17, no. 11, pp. 3666–3679, 2024.

[59] V. Chaoji, S. Ranu, R. Rastogi, and R. Bhatt, "Recommendations to boost content spread in social networks," in *Proceedings of the 21st international conference on World Wide Web*, 2012, pp. 529–538.

[60] S. Huang, W. Lin, Z. Bao, and J. Sun, "Influence maximization in real-world closed social networks," *Proceedings of the VLDB Endowment*, vol. 16, no. 2, pp. 180–192, 2022.

[61] S. B. Seidman, "Network structure and minimum degree," *Social networks*, vol. 5, no. 3, pp. 269–287, 1983.

[62] V. Batagelj and M. Zaversnik, "An o (m) algorithm for cores decomposition of networks," *arXiv preprint cs/0310049*, 2003.

[63] J. Cohen, "Trusses: Cohesive subgraphs for social network analysis," *National security agency technical report*, vol. 16, no. 3.1, pp. 1–29, 2008.

[64] K. Saito, T. Yamada, and K. Kazama, "Extracting communities from complex networks by the k-dense method," *IEICE Transactions on Fundamentals of Electronics, Communications and Computer Sciences*, vol. 91, no. 11, pp. 3304–3311, 2008.

[65] Y. Fang, Z. Wang, R. Cheng, H. Wang, and J. Hu, "Effective and efficient community search over large directed graphs," *IEEE Transactions on Knowledge and Data Engineering*, vol. 31, no. 11, pp. 2093–2107, 2018.

[66] W. Chen, C. Wang, and Y. Wang, "Scalable influence maximization for prevalent viral marketing in large-scale social networks," in *Proceedings of the 16th ACM SIGKDD international conference on Knowledge discovery and data mining*, 2010, pp. 1029–1038.

[67] O. Amini, D. Peleg, S. Pérennes, I. Sau, and S. Saurabh, "On the approximability of some degree-constrained subgraph problems," *Discrete Applied Mathematics*, vol. 160, no. 12, pp. 1661–1679, 2012.

[68] M. Mitzenmacher and E. Upfal, *Probability and computing: Randomization and probabilistic techniques in algorithms and data analysis*. Cambridge university press, 2017.

[69] L. Breiman, "Random forests," *Machine learning*, vol. 45, pp. 5–32, 2001.

[70] P. Cunningham and S. J. Delany, "K-nearest neighbour classifiers-a tutorial," *ACM computing surveys (CSUR)*, vol. 54, no. 6, pp. 1–25, 2021.

[71] V. G. Costa and C. E. Pedreira, "Recent advances in decision trees: An updated survey," *Artificial Intelligence Review*, vol. 56, no. 5, pp. 4765–4800, 2023.

[72] S. Zhang, J. Sun, W. Lin, X. Xiao, Y. Huang, and B. Tang, "Information diffusion meets invitation mechanism," in *Companion Proceedings of the ACM on Web Conference 2024*, 2024, pp. 383–392.

[73] J. Kunegis, "Konect: the koblenz network collection," in *Proceedings of the 22nd international conference on world wide web*, 2013, pp. 1343–1350.

[74] J. Leskovec and A. Krevl, "Snap datasets: Stanford large network dataset collection," 2014, http://snap.stanford.edu/data.

[75] M. Simpson, F. Hashemi, and L. V. Lakshmanan, "Misinformation mitigation under differential propagation rates and temporal penalties," *Proceedings of the VLDB Endowment*, vol. 15, no. 10, pp. 2216–2229, 2022.

APPENDIX

A. Aggregation Functions Extensions

In this section, we extend our problem and techniques to other aggregation functions, such as *max*, *min*, and *sum*. Specifically, the influenced expectation of a MIC is defined as the minimum, maximum, or sum of the influenced expectations of the nodes in that community. **(1)** For the max function in disease prevention, a "super-spreader" with the maximum influenced expectation can significantly increase the community's overall infection risk, as one highly influenced individual can impact the entire community. **(2)** For the min function, in a marketing campaign, the success of promoting a product relies on the purchasing desire of every community member, and the minimum influenced expectation ensures that all members of the community are engaged. **(3)** For the sum function, the total purchase probability of all community members in a marketing campaign reflects the overall demand for a product, indicating the potential market capacity.

Under the max and sum functions, the MIC straightforwardly corresponds to the maximal D-core in the initial graph G, provided the size of maximal D-core is larger than γ. Therefore, we focus on the minimum function. We begin with a modified definition of the influenced expectation of a subgraph H of G under the min function.

Definition 6. (Influenced expectation of H under min function). *Given a subgraph $H(V_H, E_H) \subseteq G$, a node set $S \subset V$, and an influence propagation model M, we denote the influenced expectation of H as $Ie(H,S) = \min_{v \in H_v} Ie(v,S)$, which represents the probability that H is influenced by S under propagation model M.*

It can be verified that the MIC defined in Definition 4 is also suitable for the above definition. Then, we extend our GlobalSearch and LocalSearch to solve the MICS problem under the min function based on the following Lemmas.

Lemma 1. *For any community C, if we delete the node with the smallest influenced expectation in C and the resulting subgraph still contains a community C', then the influenced expectation of C' is no smaller than that of C.*

Lemma 2. *Given an empty subgraph G', we add nodes from the maximal D-core of G to G' in descending order of their influenced expectations until G' contains a MIC C'. The influenced expectation of C' is then the maximal.*

The proofs of the above two Lemmas are straightforward, thus, we omit them here. Based on Lemma 1, our GlobalSearch algorithm can directly extend to solve the MICS problem under the min function. Then, we extend our LocalSearch algorithm based on Lemma 2 and propose the LocalSearch-min algorithm. The main ideas of this algorithm are as follows. We construct a subgraph G' by gradually adding nodes in descending order of their influenced expectations from the maximal D-core in original graph G, until a maximal connected subgraph is formed. This subgraph should be larger than γ and each node in it must satisfy the (k,l) constraint. Then, this connected subgraph is recognized as the MIC with the maximum influenced expectation. The pseudo-code of the LocalSearch-min algorithm is presented in Algorithm 5. Since it is easy to follow, we omit the detailed explanation here.

Algorithm 5 LocalSearch-min

Input: a graph $G(V_G, E_G)$, two parameters k and l, a size constraint γ, the influenced expectation $Ie(v,S)$ for $\forall v \in V_G$
Output: the most influenced community MIC with $MIC \geq \gamma$

Compute the maximal D-core D of G;
Sort all nodes v of D's connected components $D' \subseteq D$ with $|D_i| \geq \gamma$ in descending order of $Ie(v,S)$ and mark them as unvisited;
$G' \leftarrow \emptyset$;
for each $v \in D$ **do**
  if v is unvisited **then**
    Add u into G' and mark v as visited;
  compute $\tilde{D}$-core D' of G';
  for each connected component D'_i of D' **do**
    if $|D'_i| \geq \gamma \wedge Ie(D'_i, S) > Ie(MIC, S)$ **then**
      $MIC \leftarrow D'_i$;
Return MIC;

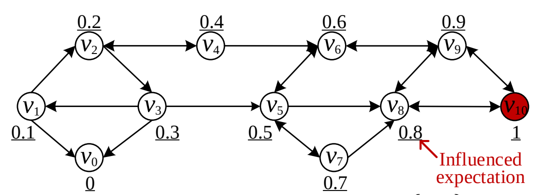

Fig. 10: An example graph with $S = \{v_{10}\}$

Time Complexity. Following the time complexity analyzes of Algorithm 2, after adding each node u into G', the complexity of searching for the MIC is $O(|V_G| + |E_G|)$. Therefore, the total time complexity of Algorithm 5 is $O(|V_G| \cdot (|V_G| + |E_G|))$.

B. Proof of Theorem 5

Proof. Consider the graph in Figure 10. Let $\gamma = 2$; $k = 1$; $l = 1$.

Non-monotonicity. Let H_1 be the subgraph induced by vertices $\{v_6, v_9\}$; H_2 be the subgraph induced by vertices $\{v_5, v_6, v_9\}$; H_3 be the subgraph induced by vertices $\{v_5, v_6\}$. We have the following inequalities: (1) $Ie(H_1, v_{10}) = (0.6 + 0.9)/2 = 0.75 > Ie(H_2, v_{10}) = (0.5 + 0.6 + 0.9)/3 = 0.67$, and (2) $Ie(H_3, v_{10}) = 0.55 < Ie(H_2, v_{10}) = 0.67$. Obviously, $Ie(H,S)$ is non-monotonic.

Non-submodularity. For two arbitrary sets X and Y, if a function $f(\cdot)$ is submodular, it must satisfy $f(X) + f(Y) \geq f(X \cup Y) + f(X \cap Y)$. Let H_4 be the subgraph induced by vertices $\{v_8, v_9, v_{10}\}$. Then, $Ie(H_4, v_{10}) = 0.9$; $Ie(H_2 \cup H_4, v_{10}) = 0.76$; $Ie(H_2 \cap H_4, v_{10}) = 0.9$. We have the following inequality: $Ie(H_2, v_{10}) + Ie(H_4, v_{10}) = 0.67 + 0.9 = 1.57 < Ie(H_2 \cup H_4, v_{10}) + Ie(H_2 \cap H_4, v_{10}) = 0.76 + 0.9 = 1.66$. Therefore, $Ie(H,S)$ is non-submodular. $\square$

C. Proof of Theorem 6

Proof. Applying chernoff inequalities, we have $\Pr[\tilde{Ie}(v,S) \cdot |\mathcal{I}| - |\mathcal{I}| \cdot Ie(v,S) \geq \epsilon |\mathcal{I}| \cdot Ie(v,S)] \leq \exp\left(-\frac{\epsilon^2}{2+\epsilon} \cdot |\mathcal{I}| \cdot Ie(v,S)\right)$. Given $|\mathcal{I}| \geq \frac{l \cdot (2+\epsilon) \cdot \log n}{\epsilon^2 \cdot Ie(v,S)}$, we have $\Pr[\tilde{Ie}(v,S) - Ie(v,S) \geq \epsilon \cdot Ie(v,S)] \leq n^{-l}$. Thus, $|\tilde{Ie}(v,S) - Ie(v,S)| < \epsilon \cdot Ie(v,S)$ holds with probability at least $1 - n^{-l}$. $\square$

TABLE VIII: Performance of Predicting Models (Skewed seed node sets)

Model	EmailCore						WikiVote						Epinions					
	T-time	P-time	MSE	RMSE	MAE	R-Squared	T-time	P-time	MSE	RMSE	MAE	R-Squared	T-time	P-time	MSE	RMSE	MAE	R-Squared
RF	0.0573s	0.0014s	**0.0010**	**0.0316**	**0.0154**	**0.9752**	0.2743s	0.0018s	**0.0001**	**0.0117**	**0.0029**	**0.9938**	2.5600s	0.0047s	**0.0002**	**0.0164**	**0.0049**	**0.9943**
DT	0.0015s	**0.0001s**	0.0106	0.1030	0.0352	0.7375	0.0077s	**0.0001s**	0.0007	0.0282	0.0066	0.9645	0.0815s	**0.0002s**	0.0019	0.0446	0.0105	0.9580
KNN	**0.0003s**	0.0006s	0.0034	0.0589	0.0213	0.9141	**0.0004s**	0.0008s	0.0003	0.0198	0.0046	0.9825	**0.0015s**	0.0028s	0.0008	0.0283	0.0071	0.9831

Model	Pokec						Livejournal						WikiLink					
	T-time	P-time	MSE	RMSE	MAE	R-Squared	T-time	P-time	MSE	RMSE	MAE	R-Squared	T-time	P-time	MSE	RMSE	MAE	R-Squared
RF	701.65s	0.0964s	**6.29E-05**	**0.0079**	**0.0031**	**0.9909**	2241.8s	0.5089s	**5.26E-05**	**0.0072**	**0.0023**	**0.9891**	6309.8s	1.4454s	**6.47E-05**	**0.0080**	**0.0018**	**0.9919**
DT	21.906s	**0.0024s**	0.0005	0.0229	0.0093	0.9238	70.219s	**0.0119s**	0.0003	0.0198	0.0064	0.9186	200.98s	**0.0393s**	0.0004	0.0209	0.0044	0.9452
KNN	**0.0433s**	0.0535s	0.0002	0.0139	0.0052	0.9720	**0.1142s**	0.1664s	0.0001	0.0122	0.0036	0.9692	**0.1715s**	0.4785s	0.0002	0.0150	0.0027	0.9716

TABLE IX: Performance of Predicting Models (Random seed node sets)

Model	Epinions						Slashdot						Livejournal					
	T-time	P-time	MSE	RMSE	MAE	R-Squared	T-time	P-time	MSE	RMSE	MAE	R-Squared	T-time	P-time	MSE	RMSE	MAE	R-Squared
RF	4.0114s	0.0043s	**2.57E-05**	**0.0050**	**0.0006**	**0.9751**	4.4609s	0.0046s	**3.73E-05**	**0.0061**	**0.0009**	**0.9891**	10729.8s	0.5085s	**1.95E-05**	**0.0044**	**0.0002**	**0.8682**
DT	0.1152s	**0.0002s**	0.0017	0.0423	0.0059	-0.7350	0.1282s	**0.0002s**	0.0016	0.0400	0.0044	-0.7656	476.21s	**0.0121s**	0.0002	0.0162	0.0010	-0.7709
KNN	**0.0015s**	0.0028s	0.0016	0.0410	0.0058	-0.6261	**0.0016s**	0.0029s	0.0014	0.0383	0.0042	-0.6189	**0.1139s**	0.1628s	0.0001	0.0130	0.0008	-0.1363

TABLE X: Effect of Parameters of Random Forest model

$\lvert S\rvert$	EmailCore					$\lvert S\rvert$	Pokec					$\lvert S\rvert$	Livejournal					$\lvert S\rvert$	WikiLink				
	MD	MSL	MSS	NE	MSE		MD	MSL	MSS	NE	MSE		MD	MSL	MSS	NE	MSE		MD	MSL	MSS	NE	MSE
10	None	1	5	50	0.0154	**100**	None	4	5	100	0.0028	**100**	10	1	10	50	0.0021	**100**	10	1	5	50	0.0021
20	None	1	10	50	0.0028	**200**	10	1	2	50	0.0029	**200**	10	1	2	100	0.0021	**200**	None	1	5	50	0.0029
30	None	1	5	50	0.0188	**300**	10	1	5	100	0.0051	**300**	10	1	10	50	0.0035	**300**	None	1	10	50	0.0035
40	20	2	5	50	0.0207	**400**	10	4	5	50	0.0060	**400**	10	1	5	50	0.0042	**400**	None	1	2	100	0.0042
50	20	1	5	50	0.0249	**500**	20	1	10	50	0.0067	**500**	None	1	2	100	0.0048	**500**	None	1	5	100	0.0048

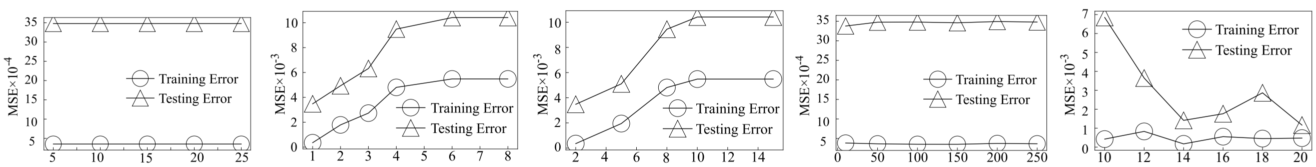

(a) MD (b) MSL (c) MSS (d) NE (e) Samle size

Fig. 11: Fit Analysis of Random Forest Model

D. Proof of Theorem 7

Proof. As $Ie(D_1, S) > \max_{v \in V_{D_2}} Ie(v, S)$ and $D_3 \subseteq D_2$, it holds that $Ie(D_1, S) > \max_{v \in V_{D_3}} Ie(v, S)$. Thus, $Ie(D_1, S) > Ie(D_3, S)$. □

E. Detailed Time Complexity of L-InfExp

L-InfExp consists of four main components: training data preparation (i.e., $\mathcal{S}$ and $\mathcal{E}$), feature encoding (i.e., X and Y), model training, and online predicting. Let β denote the size of the training data, i.e., $|\mathcal{E}| = |\mathcal{S}| = \beta$. The complexity of each component is as follows: **(i)** Training data preparation: Based on the complexity of S-InfExp analyzed in Section V-A, computing the influenced expectations $\mathcal{E}$ for $\mathcal{S}$ takes $O(\beta \cdot \alpha \cdot |V_G| \log(|V_G|))$ time. **(ii)** Feature encoding: The total complexity for encoding all seed node sets in $\mathcal{S}$ is $O(\beta \cdot |V_G|)$. Similarly, encoding all influenced expectation sets $\mathcal{E}$ also takes $O(\beta \cdot |V_G|)$. Constructing the multi-hot matrices X and Y requires $O(\beta \cdot |V_G|)$ time, resulting in an overall complexity of $O(\beta \cdot |V_G|)$ for the feature encoding. **(iii)** Model training: The complexity of training a random forest model is $O(T \cdot \beta \cdot \sqrt{|V_G|} \cdot d)$, where T and d are hyperparameters of the random forest model, with T representing the number of trees and d representing the depth of the trees. Thus, the overall complexity of the offline model training stage of L-InfExp is $O(\beta \cdot \alpha \cdot |V_G| \log(|V_G|)) + O(\beta \cdot |V_G|) + O(T \cdot \beta \cdot \sqrt{|V_G|} \cdot d)$. **(iv)** Online predicting: the complexity of encoding the seed node set S is $O(|V_G|)$, and the complexity of the prediction using the trained model is $O(T \cdot |V_G| \cdot d)$. Thus, the total complexity for the online prediction phase is $O(|V_G|) + O(T \cdot |V_G| \cdot d)$.

F. Full Experimental Results

This section shows the complete experiment results that are omitted in Section VII due to space constraints.

Performance of predictive models. In this experiment, we compare RF, DT, and KNN model on skewed seed node sets and random seed node sets. For each model, we report both *training time* (T-time) and *prediction time* (P-time), as well as *predictive accuracy* using four metrics: *Mean Squared Error* (MSE), *Root Mean Squared Error* (RMSE), *Mean Absolute Error* (MAE), and *R-squared*. For MSE, RMSE, and MAE, lower values indicate better performance. For R-squared, higher values are preferred. The results, summarized in Table VIII and Table IX, show that, for both skewed seed node sets and random seed node sets, RF delivers the best predictive accuracy among the three models, with the smallest disparity between predicted and actual influenced expectations.

Effect of hyperparameters on RF model. We study the impact of various hyperparameters combinations on RF performance as the number of seed nodes $|S|$ varies. The four hyperparameters tested are MD in {None, 10, 20}, MSL in {1, 2, 4}, MSS in {2, 5, 10}, and NE in {50, 100, 200}. A grid search is used to evaluate performance by testing all possible combinations of these hyperparameter and employing cross-validation to identify the best performing set. The optimal hyperparameter combinations for different $|S|$ values across different datasets are presented in Table X. It can be observed that, smaller MSL and MSS values generally improve performance by producing more complex decision trees, which fit the data more accurately, while MD and NE have a much smaller impact on the model's accuracy.

Fit analysis of RF model. We conduct a fit analysis experiment of the RF model on the *Epinions* by varying MD, MSL, MSS, NE, and sample size. We use 50% of the samples for training and the remaining 50% for testing, with MSE as the evaluation metric. Results are plotted in Figure 11. We observe that increasing MSL and MSS leads to higher training and testing errors, indicating that reduced model complexity decreases fit quality. Additionally, increasing MD and NE has little effect on training or testing errors. Furthermore, a larger sample size improves model stability and generalization ability, as evidenced by lower testing errors.

Effect of $|S|$. We analyze how the number of seed nodes $|S|$ affects running time. Results are shown in Figures 12(a)-19(a). We observe that the running times of M-InfExp and S-InfExp increase with $|S|$, as they need to generate more influence propagation instances. Therefore, M-InfExp and S-InfExp takes more time to generate influence propagation instances, resulting in higher running time. In addition, it can be seen that S-InfExp runs faster than M-InfExp because S-InfExp skips certain nodes when sampling influence propagation instances, thereby improving sampling efficiency. L-InfExp, on the other hand, maintains a relatively stable and lower running time. This is because, for online influenced expectation prediction, S-InfExp encodes S into a multi-hot vector $\boldsymbol{x}_S \in \{0,1\}^n$, so its performance is less sensitive to the changes in $|S|$. Moreover, the running times of NeiborSearch, GlobalSearch, and LocalSearch remain relatively stable with $|S|$ since this parameter mainly influences the computation of influenced expectations. LocalSearch is significantly faster than GlobalSearch and NeiborSearch across all settings, representing the high efficiency of our LocalSearch.

Effect of γ. We investigate the impact of the size constraint γ on algorithm performance. Figures 12(b)-19(b) show the results. We can observe that increasing γ has little effect on running time across all algorithms for influenced expectation computation. This is because γ only affects the size of the returned community, not the computation of influenced expectations. Moreover, the running time of LocalSearch decreases as the γ increases. This is because a larger γ leads to newly generated connected components that are less likely to satisfy the size condition, thereby reducing the number of communities that need to be examined. However, both NeiborSearch and LocalSearch show a slight increase in running time with larger γ. This is due to the fact that in the SearchLocalMIC algorithm, more vertices need to be inserted to search for the local most influenced community that meets the larger size condition, resulting in increased time required to compute the D-core and traverse all connected components.

Effect of k and l. We evaluate the effects of parameters k and l on algorithm performance. Figures 12(c)-19(c) present the results for k. Figures 12(d)-19(d) present the results for l. As k (or l) increases, the running time for NeiborSearch, GlobalSearch, and LocalSearch decreases because a larger k results in a smaller D-core, reducing the number of nodes that need to be processed. The running times of M-InfExp, S-InfExp, and L-InfExp remain unchanged as k and l only impact the community search.

Scalability. We assess the scalability of our algorithms by varying the graph size. To this end, we randomly select a certain number of nodes from the graph to form the induced subgraph and test the running time of all algorithms. Figure 20 illustrates that the running times of M-InfExp, S-InfExp, NeiborSearch, GlobalSearch, and LocalSearch increase as the graph size grows. This is because NeiborSearch, GlobalSearch, and LocalSearch require more time to identify communities in larger graphs. For M-InfExp and S-InfExp, the increased running time is mainly due to the larger size of influence propagation instances. The running time of L-InfExp remains stable, as the efficiency of this learning based algorithm is not sensitive to the graph size.

Finally, we provide some experimental results on random seed node sets.

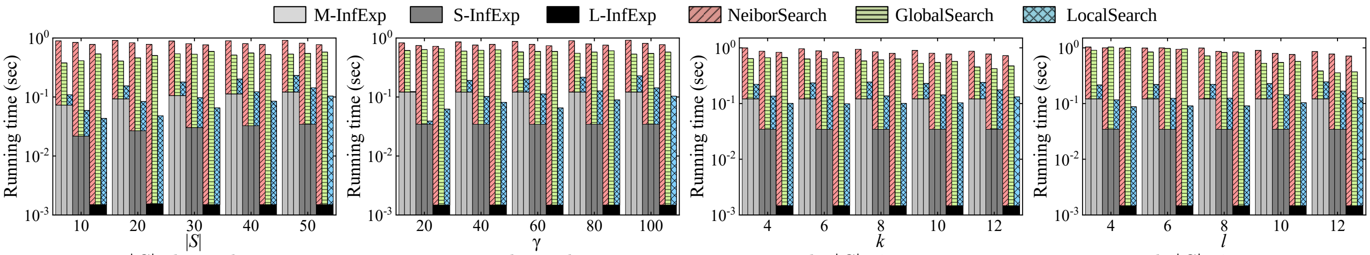

(a) vs. $|S|$ (k=10, l=10) (b) vs. γ (k=10, l=10) (c) vs. k ($|S|$=50, γ=100) (d) vs. l ($|S|$=50, γ=100)

Fig. 12: Running time on EmailCore

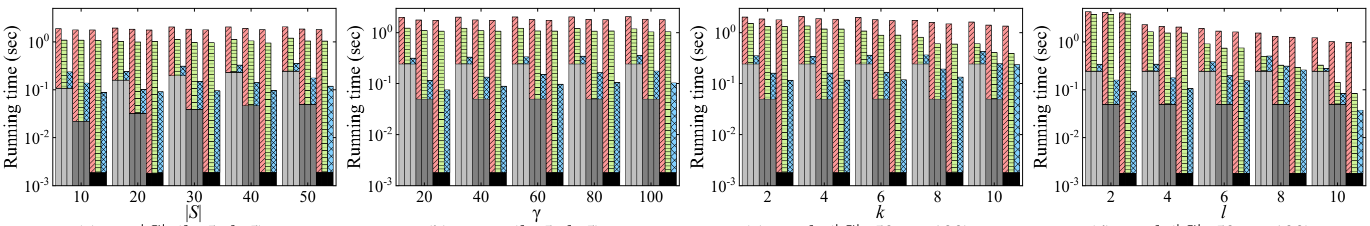

(a) vs. $|S|$ (k=5, l=5) (b) vs. γ (k=5, l=5) (c) vs. k ($|S|$=50, γ=100) (d) vs. l ($|S|$=50, γ=100)

Fig. 13: Running time on WikiVote

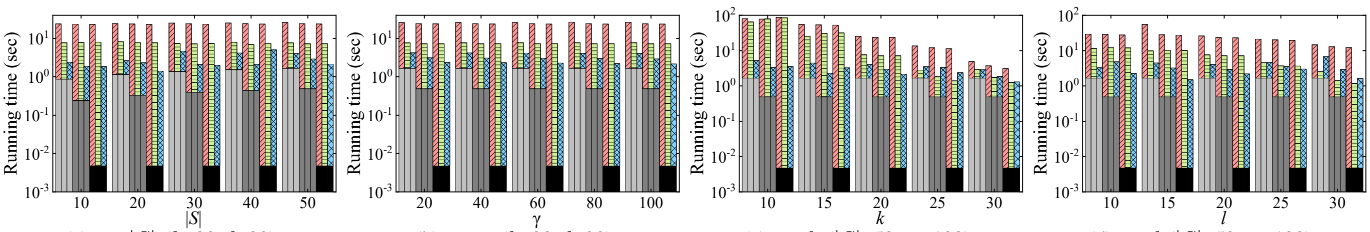

(a) vs. $|S|$ (k=20, l=20) (b) vs. γ (k=20, l=20) (c) vs. k ($|S|$=50, γ=100) (d) vs. l ($|S|$=50, γ=100)

Fig. 14: Running time on Epinions

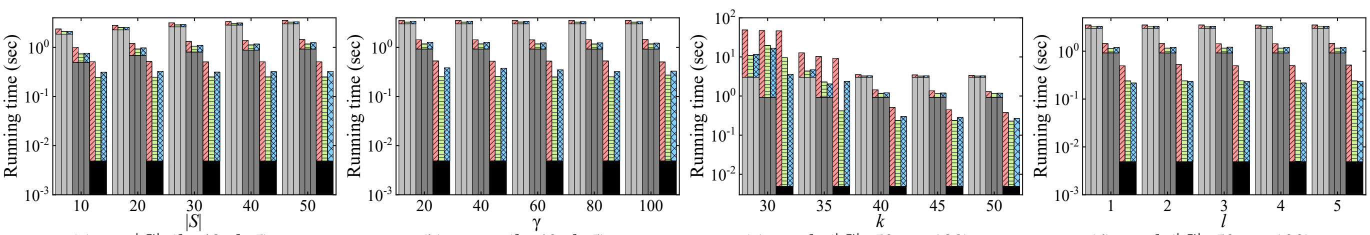

(a) vs. $|S|$ (k=40, l=5) (b) vs. γ (k=40, l=5) (c) vs. k ($|S|$=50, γ=100) (d) vs. l ($|S|$=50, γ=100)

Fig. 15: Running time on Slashdot

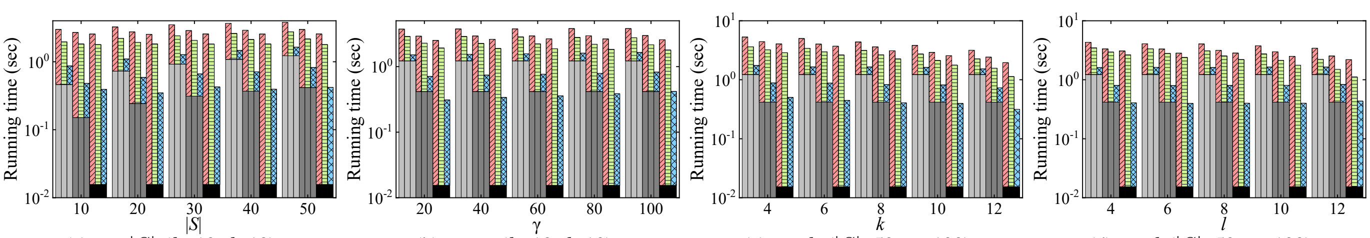

(a) vs. $|S|$ (k=10, l=10) (b) vs. γ (k=10, l=10) (c) vs. k ($|S|$=50, γ=100) (d) vs. l ($|S|$=50, γ=100)

Fig. 16: Running time on EmailEuall

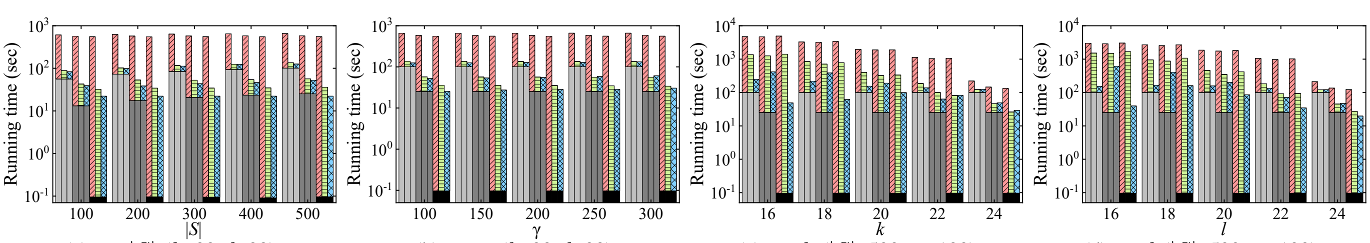

(a) vs. $|S|$ (k=22, l=22) (b) vs. γ (k=22, l=22) (c) vs. k ($|S|$=500, γ=100) (d) vs. l ($|S|$=500, γ=100)

Fig. 17: Running time on Pokec

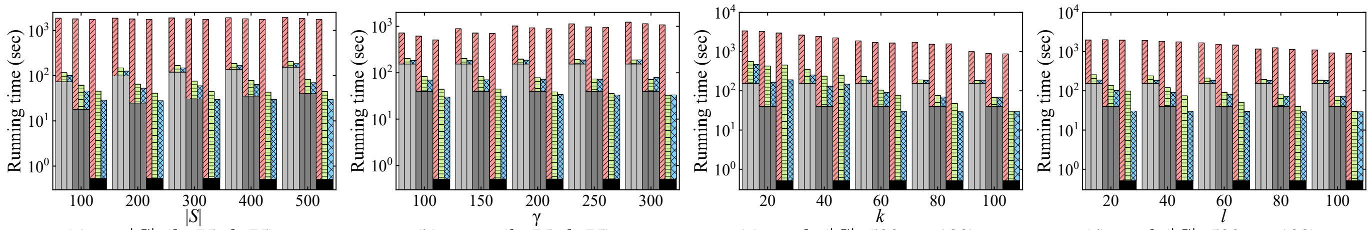

(a) vs. $|S|$ (k=75, l=75) (b) vs. γ (k=75, l=75) (c) vs. k ($|S|$=500, γ=100) (d) vs. l ($|S|$=500, γ=100)

Fig. 18: Running time on Livejournal

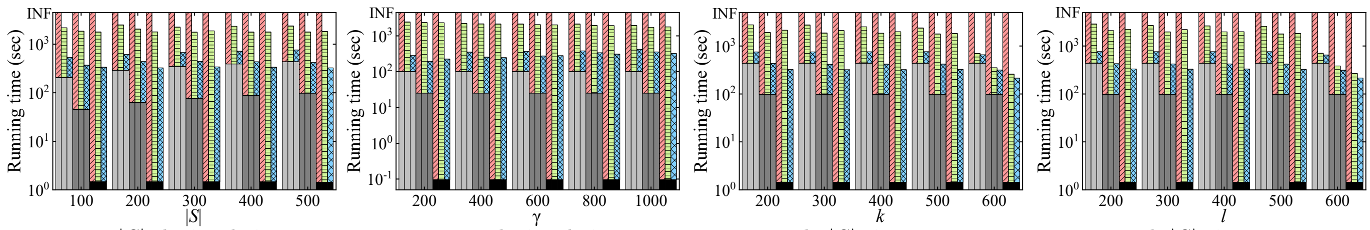

(a) vs. $|S|$ (k=500, l=500) (b) vs. γ (k=500, l=500) (c) vs. k ($|S|$=500, γ=100) (d) vs. l ($|S|$=500, γ=100)

Fig. 19: Running time on WikiLink

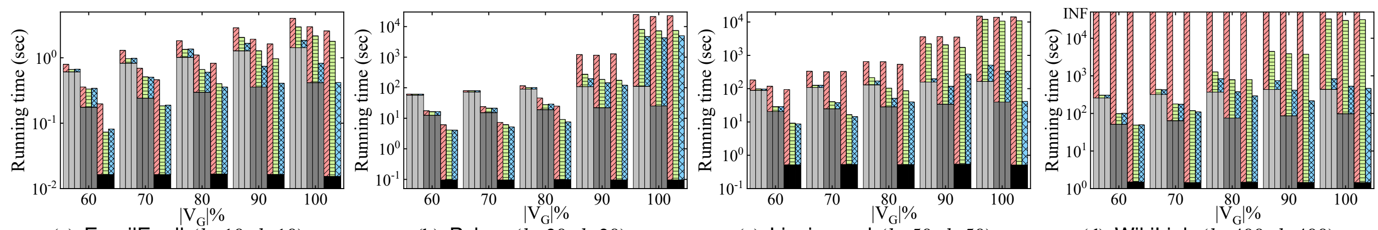

(a) EmailEuall (k=10, l=10) (b) Pokec (k=20, l=20) (c) Livejournal (k=50, l=50) (d) WikiLink (k=400, l=400)

Fig. 20: Scalability testing

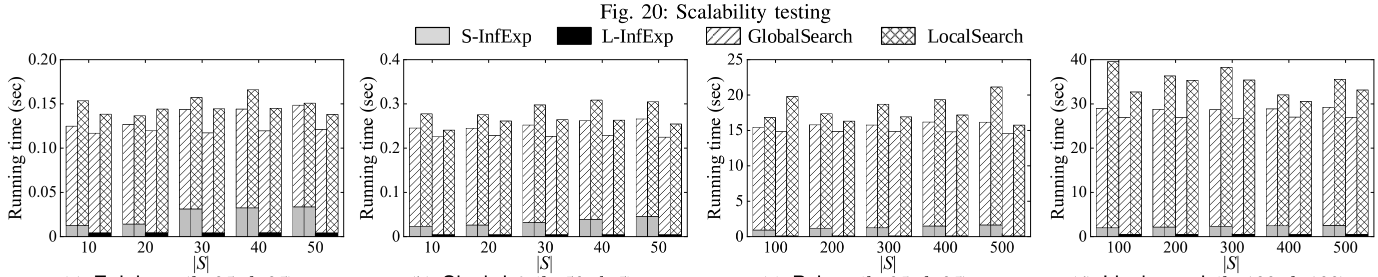

(a) Epinions (k=35, l=35) (b) Slashdot (k=50, l=5) (c) Pokec (k=25, l=25) (d) Livejournal (k=100, l=100)

Fig. 21: Running time vs. $|S|$ (Random seed node sets)

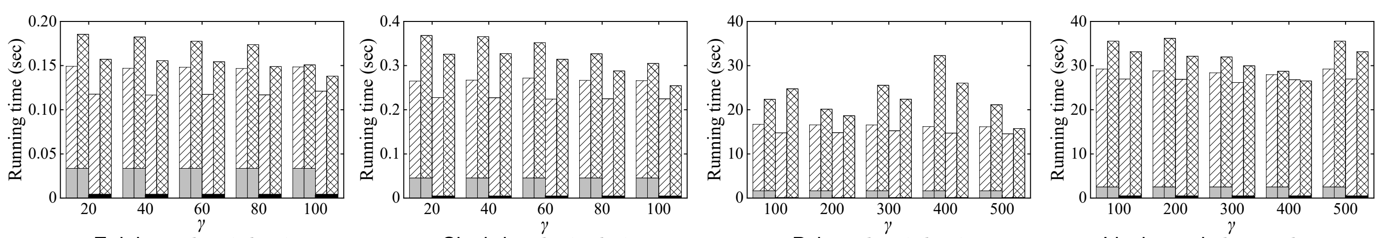

(a) Epinions (k=35, l=35) (b) Slashdot (k=50, l=5) (c) Pokec (k=25, l=25) (d) Livejournal (k=100, l=100)

Fig. 22: Running time vs. γ (Random seed node sets)

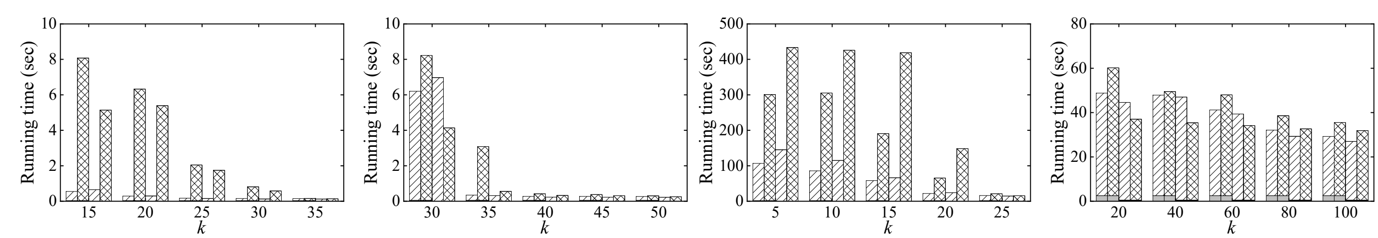

(a) Epinions ($|S|$=50, γ=100) (b) Slashdot ($|S|$=50, γ=100) (c) Pokec ($|S|$=500, γ=100) (d) Livejournal ($|S|$=500, γ=100)

Fig. 23: Running time vs. k (Random seed node sets)